

Biofuel from hydrocracking of *Cerbera manghas* oil over Ni-Zn/HZSM-5 catalyst

Lenny Marlinda^{1†}, Danawati Hari Prajitno^{2†}, Achmad Roesyadi^{2†}, Ignatius Gunardi^{2†}, Yustia Wulandari Mirzayanti^{3†}, Muhammad Al Muttaqii^{4†}, Agus Budiarto^{3†}

1. University of Jambi, Department of Chemistry, Jambi, Indonesia.
2. Sepuluh Nopember Institute of Technology, Department of Chemical Engineering, Surabaya, Indonesia.
3. Adhi Tama Institute of Technology, Department of Chemical Engineering, Surabaya, Indonesia.
4. Indonesian Institute of Sciences, Research Center for Chemistry, Tangerang Selatan, Indonesia.

+Corresponding author: Lenny Marlinda, **Phone:** +62 81366079067, **Email address:** marlindalenny@unja.ac.id

ARTICLE INFO

Article history:

Received: July 26, 2020

Accepted: October 08, 2021

Published: January 01, 2022

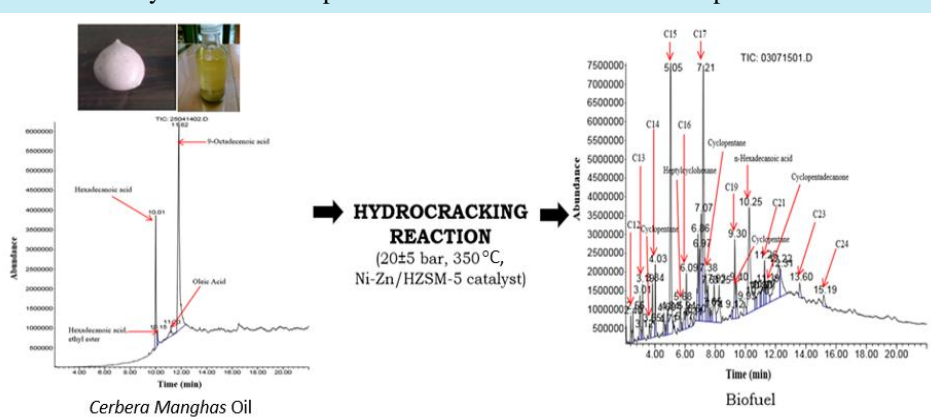
Keywords

1. the non-edible vegetable oil
2. gasoil like-hydrocarbon
3. H-ZSM-5
4. cracking

Section Editor: Assis Vicente Benedetti

ABSTRACT: The effects of reaction temperature on the hydrocarbon composition of biofuel produced in hydrocracking of *Cerbera manghas* oil with Ni-Zn/HZSM-5 catalyst were investigated. The incipient wetness impregnation method was applied to prepare the Ni-Zn/HZSM-5 catalysts. Furthermore, the properties of catalysts were measured by X-ray diffraction, atomic absorption spectrometry, and nitrogen physisorption. Hydrocracking process was carried out in Parr USA pressure batch reactor at pressure of 20 ± 5 bar after flowing H_2 for 1 h. The reaction with a catalyst/oil ratio of 1 g/150 mL proceeded at various temperatures of 350, 375 and 400 °C for 2 h. Gas chromatography-mass spectrometry was used to analyze biofuel. The most abundant hydrocarbon compounds in biofuel were identified as pentadecane and heptadecane (a major diesel fuel compound) with a different amount at different reaction temperatures. It can be said that the

hydrodecarboxylation/decarbonylation routes were the predominant reaction pathways and oxygen removal occurred during hydrocracking. The *Cerbera manghas* oil can be recommended as a promising biofeed to produce the gasoil as an alternative transportation fuel.



1. Introduction

When liquid fuel from fossil sources was applied as transportation fuel, the increasing CO₂ emission rapidly increased. The use of biofuel will be the right step to achieve zero waste. Hydrocarbon compounds in biofuel are similar with petroleum diesel fuel so that biofuel can be a substitute for diesel fuel. Development of biofuel production technology continues to evolve concurrently with the exploration of vegetable oil as raw materials while maintaining the sustainability of food security. Biofuel was already used both in pure form and blending is fatty acid methyl esters (FAMEs), also known as oxygenated biofuels, as reported by [Romero et al. \(2015\)](#). The oxygenated biofuel is also known as biodiesel. Bio-oil and biodiesel can be grouped as biofuels, which are environmentally friendly alternative fuels that can replace petroleum. However, they both have different hydrocarbon compositions. Biodiesel contains hydrocarbon compounds with oxygen atoms in esters. The bio-oil contains a large number of organic compounds, namely alkanes, aromatic hydrocarbons, and phenol derivatives. Small amounts of ketones, esters, ethers, sugars, amines and alcohols with an H/C molar ratio higher than 1.5 were identified in bio-oil ([Lu et al., 2009](#); [Wu et al., 2009](#)). The method of high thermal decomposition (pyrolysis) without the addition of O₂/air was used to produce it ([Isahak et al., 2012](#)).

Fatty acid methyl esters or biodiesel were produced by transesterification of the extracted seed-derived vegetable oils (e.g., rapeseed oil, cotton oil, palm oil, soybean oil, and jatropha seed) and methanol. It was still having the properties that have not been profitable for diesel engines ([Ayodele et al., 2015](#); [Chen et al., 2016](#); [Kim et al., 2013](#); [Pinto et al., 2013](#); [Šimáček et al., 2009](#); [Wang et al., 2014](#)). Some phenomena, such as blockages in some parts of the fuel system, the appearance of deposit and sludge on the storage system, corrosion on metal parts due to the relatively high-water solubility in FAMEs, causing swelling of rubber components, can be a factor causing engine damage ([Kim et al., 2013](#); [Šimáček et al., 2009](#); [2011](#)). The limiting properties of FAMEs for the application directly as a fuel in vehicle engines are low energy density, poor oxidation stability of FAMEs ([Ayodele et al., 2015](#); [Chen et al., 2016](#); [Kim et al., 2013](#)), which is caused by excess oxygen incorporated in carboxyl or carbonyl groups ([Chen et al., 2016](#); [Kim et al., 2013](#); [Romero et al., 2015](#); [Wang et al., 2014](#)), the high value of viscosity and pour point, poor calorific value ([Wang et al., 2014](#)), poor storage stability, and glycerol by-product menace ([Ayodele et al., 2015](#)). Therefore,

FAMEs composed of the different chemical compounds can damage the engine combustion and reduce the engine performance ([Pinto et al., 2013](#)).

The other method for converting vegetable oil to biofuel is hydrocracking applied before in crude oil refinery unit with heterogeneous catalyst. Some of the catalysts have been applied in vegetable oils processing into biofuel through the catalytic cracking and hydrocracking. The CoMoS and NiMoS catalysts ([Kim et al., 2013](#); [Zhang et al., 2014](#)), NiMo/ZSM-5-alumina ([Ishihara et al., 2014](#)), CoMo/ γ -Al₂O₃ ([Bezergianni et al., 2014](#); [Pinto et al., 2014](#); [Rasyid et al., 2015](#)), ultra-stable Y (USY) zeolite ([Li et al., 2014](#)), HZSM-5 based catalyst, e.g., Ni or Zn supported on HZSM-5 ([Budianto et al., 2014a](#); [Roesyadi et al., 2013](#)), Pt, Pd, or Au supported on H-ZSM-5 ([Budianto et al., 2014b](#)), Ni-Zn/HZSM-5 ([Prajitno et al., 2015](#)), Ni or Ga supported on HZSM-5 ([Tamiyakul et al., 2016](#)) were typical catalysts for catalytic cracking or hydrocracking of triglycerides to obtain biofuel. However, the mesoporous zeolite is preferred to support diffusion of the reactants and produce alkane isomers with relatively high yields ([Chen et al., 2016](#)).

[Wang et al. \(2014\)](#) deoxygenated soybean oil with the Ni/HZSM-5 catalyst through a single-step hydrotreatment process combining deoxygenation of fatty acid into n-paraffin as the main hydrocarbon product and isomerization to obtain isoparaffin. Apparently, catalytic activity of Ni/SAPO-11 is higher than Ni/HZSM-5 catalyst in a single-step hydrotreatment process based on the amount of n-paraffin produced and oxygenated compounds remaining. Hierarchical pore structure becomes a good solution to obtain the size of micropores-mesopores on HZSM-5 in an effort to increase the activity of catalyst, as suggested by [Liu et al. \(2015\)](#). With the Ni/HZSM-5 catalyst, [Chen et al. \(2016\)](#) promoted long-chain unsaturated FAMEs through one-step catalytic hydroprocessing (including deoxygenation and decarboxylation or decarbonylation, followed by isomerization). With the Ni/HZSM-5 catalyst (silica to alumina ratio of 25) and metal loading of 10 wt.%, it was found that high selectivity of C₅-C₁₈ n-paraffins and isomerization selectivity were 88.2 and 27.0%, respectively ([Chen et al., 2016](#)). In this case, changes in the Si/Al ratio affect the acidity of the zeolite and have an impact on variations in the composition of hydrocarbon compounds in the liquid product. Based on this, it is remarkably interesting for impregnating double promoter of Ni and Zn metal into HZSM-5 zeolite. This prepared catalyst is expected to improve the degree of triglycerides hydrocracking when compared to using one active metal only.

So far, the fuel produced has characteristics which can maintain the machine durability and do not require substantial modification of conventional machines. Problems resulted from the use of FAMES are resolved through the removal of oxygen atoms in the fatty acid by reaction hydrocracking, i.e., hydrodecarbonylation/decarboxylation (HDC) and hydrodeoxygenation (HDO) (Arun *et al.*, 2015; Ishihara *et al.*, 2014; Kim *et al.*, 2013; Silva and Sousa, 2013; Zhang *et al.*, 2014) and then followed by isomerization. Kim *et al.* (2013) stated it is especially important to understand and control the reactions (i.e., dehydrogenation, isomerization, cyclization, and aromatization) related to the oxygen removal on triglycerides in hydrocracking process to produce biofuel with fuel properties (including cloud point and cetane number). The fuel properties were influenced by hydrocarbon composition, such as (normal, iso-) paraffin, olefins, cycloparaffin, and aromatic. These reaction routes may lead to the formation of hydrocarbons such as n-paraffins, isoparaffins, cycloparaffins, aromatics, and olefins (Kim *et al.*, 2013; Ishihara *et al.*, 2014; Zhang *et al.*, 2014). It is very important to keep the hydrogen partial pressure not too high during the hydrocracking process because it resulted in a low yield of hydrocarbons, as stated by Santillan-Jimenez and Crocker (2012).

Biofuel derived from nonedible vegetable oil through hydrocracking process is becoming a promising renewable alternative fuel in sustainable energy production. The candlenut, jatropha, rubber seed, *Cerbera manghas* seed, *Calophyllum inophyllum* have been used as sources of nonedible vegetable oils. Seeds from these plants contain toxic substances which humans cannot consume, e.g., cerberin is found in *Cerbera manghas* seed. Carlier *et al.* (2014) also reported that dry seeds of *Cerbera manghas* contained a number of compounds: cerberin, deacetyltanghinin, neriifolin, and tanghinin. *Cerbera manghas* trees, part of the ecosystem of the mangrove forests, can reach a height of 12 m. These plants can be found as urban greening plants. Their seeds contained a high level of crude Cerbera oil of approximately 46–64%.

In this work, the influence of reaction temperature for two different composition ratios of metals impregnated on HZSM-5 on the hydrocarbon composition in biofuels by hydrocracking of *Cerbera manghas* oil is discussed. It is expected that characteristics of hydrocarbon composition in the biofuel produced are similar to petroleum-based fuels. Based on gas chromatography-mass spectrometry (GC-MS) analysis, decarboxylation/decarbonylation occurred during hydrocracking was also discussed.

2. Materials and Methods

2.1 Extraction of *Cerbera manghas*

Dried fruits of *Cerbera manghas* were obtained from plant that grows in Keputih, Surabaya, Indonesia. It is also known as Bintaro plant in Java Island. *Cerbera manghas* oil was extracted from seeds through the process steps that according to previous literature, as shown in Fig. 1 (Roesyadi, 2016). At first the fruit was split and the seeds were removed from the fruit. These seeds were cleaned from the skin and obtained white oval-shaped seeds. Furthermore, the seeds were dried in the sun for 7 days. After drying, the dry seeds were chopped and extracted by hydraulic press to produce oil. Oil was stored in an airtight container to prevent oxidation, which can increase free fatty acid levels. *Cerbera manghas* oil from the hydraulic extraction process was obtained as much as 2.5 L from 6 kg of seeds. It can be said that 2 kg of Bintaro seeds produce about 0.8 L of oil. Figure 2 specify the different conditions of the seed and the obtained oil.

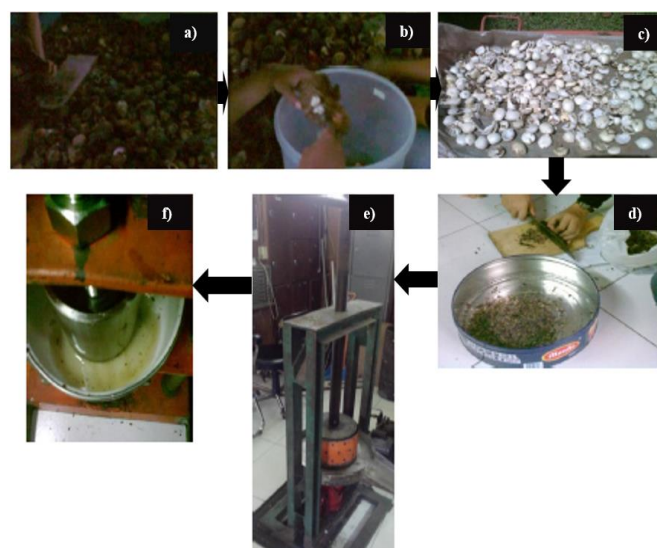


Figure 1. Extraction process of *Cerbera manghas* seeds. (a) the fruit was split into two parts, (b) the seeds were removed from the fruit, (c) the seeds were dried in the sun, (d) the dry seeds were chopped, finally (e, f) the seeds were extracted by hydraulic press.

Source: Adapted from Roesyadi (2016).



Figure 2. Different condition of *Cerbera manghas* fruit and the obtained oil. (a) a dried fruit, (b) seed with skin, (c) white oval-shaped seeds, (d) oil.

Source: Adapted from Roesyadi (2016).

2.2 Catalyst preparation

ZSM-5 zeolite in ammonium form (CBV 8014, SiO₂/Al₂O₃ ratio of 25, surface area of 400 m² g⁻¹, Na₂O of 0.05 wt.%) was provided from Zeolyst International. Meanwhile, Ni(NO₃)₂·6H₂O and Zn(NO₃)₂·6H₂O as the metal precursor were obtained from Merck with 98% purity. The calcination process on NH₄-ZSM-5 zeolite was applied to obtain HZSM-5 zeolite at temperature of 550 °C for 5 h (Sartipi *et al.*, 2013). By incipient wetness impregnation method (Haber *et al.*, 1995; Marlinda *et al.*, 2016; Sartipi *et al.*, 2013), HZSM-5 after calcined was impregnated with nickel and zinc to obtain Ni-Zn/HZSM-5 catalyst. Before impregnation, the HZSM-5 zeolite was dried overnight at a temperature of 120 °C. The amount of aqueous metal

solutions was calculated according to the total pore volume of HZSM-5 as support, which was obtained from Brunauer–Emmett–Teller (BET) analysis, as shown in Table 1. After preparing aqueous metal solutions, firstly the amount of aqueous Ni(NO₃)₂·6H₂O solution of 1.81 mol L⁻¹ was sprayed slowly to HZSM-5 zeolite while stirring and then kept overnight in a desiccator. Finally, this catalyst was dried at 120 °C for 12 h. Furthermore, in the same way as before, the amount of aqueous Zn(NO₃)₂·6H₂O solution of 1.62 mol L⁻¹ was sprayed slowly to HZSM-5 zeolite while stirring. Before drying at temperature of 120 °C for 12 h, the catalyst was kept overnight in a desiccator. Catalysts containing Ni and Zn salt solution were calcined with air at temperature of 400 °C for 2 h. After calcination, active metal usually exists as a form of metal oxide (Kim *et al.*, 2013; Romero *et al.*, 1998). The metallic phases of Ni and Zn were obtained by reducing the metal oxides under flowing hydrogen at a temperature of 450 °C for 3 h. By atomic absorption spectrometry, the metal content was 5.43 wt.% of Ni and 1.23 wt.% of Zn of the total catalyst weight. The catalyst is denoted as Ni(5.43%)-Zn(1.23%)/HZSM-5 catalyst. Other prepared catalyst is Ni(5.42%)-Zn(1.11%)/HZSM-5.

Table 1. The characterization of H-ZSM-5 and Ni-Zn/HZSM-5 catalyst.

| Catalyst | Surface area (m ² g ⁻¹) | | | Volume (cm ³ g ⁻¹) | | | D ^f (nm) | Actual metal content ^g (wt.%) | | References |
|----------------------------|--|--------|-------|---|--------------------|-------------------|---------------------|--|------|---------------------------------|
| | Total ^a | Micro | Meso | Total ^c | Micro ^d | Meso ^e | | Ni | Zn | |
| HZSM-5 | 362.77 | 315.13 | 47.64 | 0.245 | 0.156 | 0.089 | 2.709 | - | - | Present study |
| Ni(5.43%)-Zn(1.23%)/HZSM-5 | - | - | - | - | - | - | - | 5.43 | 1.23 | Present study |
| Ni(5.42%)-Zn(1.11%)/HZSM-5 | 246.06 | 205.52 | 40.54 | 0.191 | 0.101 | 0.090 | 3.109 | 5.42 | 1.11 | (Roesyadi <i>et al.</i> , 2016) |

a = total surface area BET; b = the surface area mesoporous and microporous obtained from the t-plot; c = total pore volume; d = micropore volume obtained from the t – plot; e = mesoporous volume = V_{meso} = V_{total} – V_{mikro}; f = average pore diameter; g = atomic absorption spectrometry (AAS) analysis.

Source: Elaborated by the authors using data from Roesyadi *et al.* (2016).

2.3 Characterization of catalyst

The various techniques used to characterize catalysts were X-ray diffraction (XRD), atomic absorption spectrometry (AAS) and N₂ adsorption-desorption. The metal contents of Ni dan Zn were confirmed with AAS. In principle, the distribution of metal on ZSM-5 is influenced by the preparation method used (Chen *et al.*, 2015). X-ray diffraction was applied to identify phase analysis and the Ni-Zn/HZSM-5 catalyst crystallinity. X-ray diffraction patterns of the solid catalyst (Phillip X-Pert diffractometer with Cu radiation K α) were

collected from 2 θ of 5–90° to identify the peak of crystalline zeolite ZSM-5. The existence of the crystalline phase of NiO, ZnO, Ni and Zn particles was confirmed from the diffraction patterns recorded on 2 θ = 30–80°.

The catalyst surface area was measured by BET calculation on Quantachrome NovaWin Version 10.0 according to the adsorption data with the relative pressure (P/Po) in range from 0.095 to 0.297 through the recording process of isotherm BET on five points. Before the measurement of nitrogen adsorption and desorption isotherms at a temperature of 77 K, the sample was outgassed for 16 h at 300 °C. The pore size

distributions were calculated using adsorption model of Barrett–Joyner–Halenda (BJH). Micropores volumes were obtained from the t-plot analysis. Total pore volumes were obtained according to the amount of nitrogen adsorbed at relative pressure about 0.99034. Mesoporous volumes were obtained from the reduction of the total pore volume by the volume of micropore.

2.4 Hydrocracking reaction

Hydrocracking reactions were carried out in the Parr USA pressure batch reactor equipped with a mechanical stirrer. *Cerbera manghas* oil of 150 mL and catalysts of 1 g were transferred in the reactor. To remove air, nitrogen was flowed into the reactor at least 30 min for purging. Depending on temperature condition, reaction pressure was changed between 15 and 25 bar after flowing H₂ for at least 1 h, as reported in previous study (Marlinda *et al.*, 2016). The reaction proceeded at various temperatures, i.e., 350, 375 and 400 °C for 2 h. After a reaction time was reached, the reactor temperature was allowed to reach room temperature. Furthermore, biofuel was analyzed by GC-MS, i.e., Agilent HP 6890 GC equipped with a capillary column, model Agilent 19091S-433 (HP-5MS, phenylmethylsiloxane of 5%). The column dimensions used have an internal diameter of 0.25 mm, film thickness of 0.25 μm and a length of 30 m. All

hydrocarbon components are identified using the Wiley275 and NIST02 mass spectral library of data. Based on GC-MS analysis, it is possible to estimate the relative percentages of hydrocarbon composition and distribution of products to their carbon numbers. According to Barrón *et al.* (2011), hydrocarbon compounds (including n-paraffin, isoparaffin, cycloparaffin, aromatic, olefin) were grouped in gasoline-like hydrocarbon (C5-C9), kerosene-like hydrocarbon (C10-C13), and gasoil-like hydrocarbon (C14-C22).

3. Results and discussion

3.1 Oil characterization

The clear yellow color of *Cerbera manghas* oil without purification was analyzed by GC-MS. Table 2 indicated that the most abundant compound in *Cerbera manghas* oil is oleic acid at 77.76 area%, which agrees with that obtained by Marlinda *et al.* (2016). Oleic acid is also the largest constituent of *Calophyllum inophyllum* oil, *Jatropha curcas* oil (Chuah *et al.*, 2016) and *Pongamia pinnata* oil (Dwivedi and Sharma, 2015), as much as 39.8 ± 0.4, 51.2 ± 0.6 and 65.3 wt.%, respectively.

Table 2. Compounds of *Cerbera manghas* oil tested by GC-MS.

| Compound | Chemical name | Molecular formula | Content (%) |
|----------------------|--------------------------------|--|-------------|
| Palmitic acid; C16:0 | Hexadecanoic acid | C ₁₅ H ₃₁ COOH | 20.29 |
| Oleic acid; C18:1 | 9-Octadecenoic acid | C ₁₇ H ₃₃ COOH | 77.76 |
| Ethyl palmitate | Hexadecanoic acid, ethyl ester | C ₁₈ H ₃₆ O ₂ | 1.95 |

Source: Elaborated by the authors using data from Prajino *et al.* (2015).

3.2 Catalysts characterization

Some different techniques were used to obtain the textural properties and metal content of the Ni-Zn/HZSM-5 catalyst. Figure 3 shows the type of adsorption isotherms classified by International of Pure Applied Chemistry (IUPAC) for HZSM-5 and Ni-Zn/HZSM-5 catalyst. It was clear that a combined pattern of type I and type IV was exhibited in Fig. 3b. The type of microporous solids owned by HZSM-5 is type I isotherm, as shown in Fig. 3a. It shows an initial curve that rises sharply at very low relative pressure, as reported in previous studies (Hao *et al.*, 2012; Sartipi *et*

al., 2013; Wang *et al.*, 2013). The mesopores and the pore size distribution calculated from the sorption isotherm can be called hysteresis. The presence of hysteresis exhibited with type IV isotherm was seen on high relative pressure of 0.65 towards 0.85, at which N₂ desorption does not pass through the adsorption original path (Hao *et al.*, 2012; Vitale *et al.*, 2013; Wang *et al.*, 2013). Nickel and zinc impregnated on support can create mesoporous sites in catalyst, so that bulky molecules can diffuse easily to the pores of catalyst, as reported in previous studies (Hao *et al.*, 2012; Vitale *et al.*, 2013; Wang *et al.*, 2013).

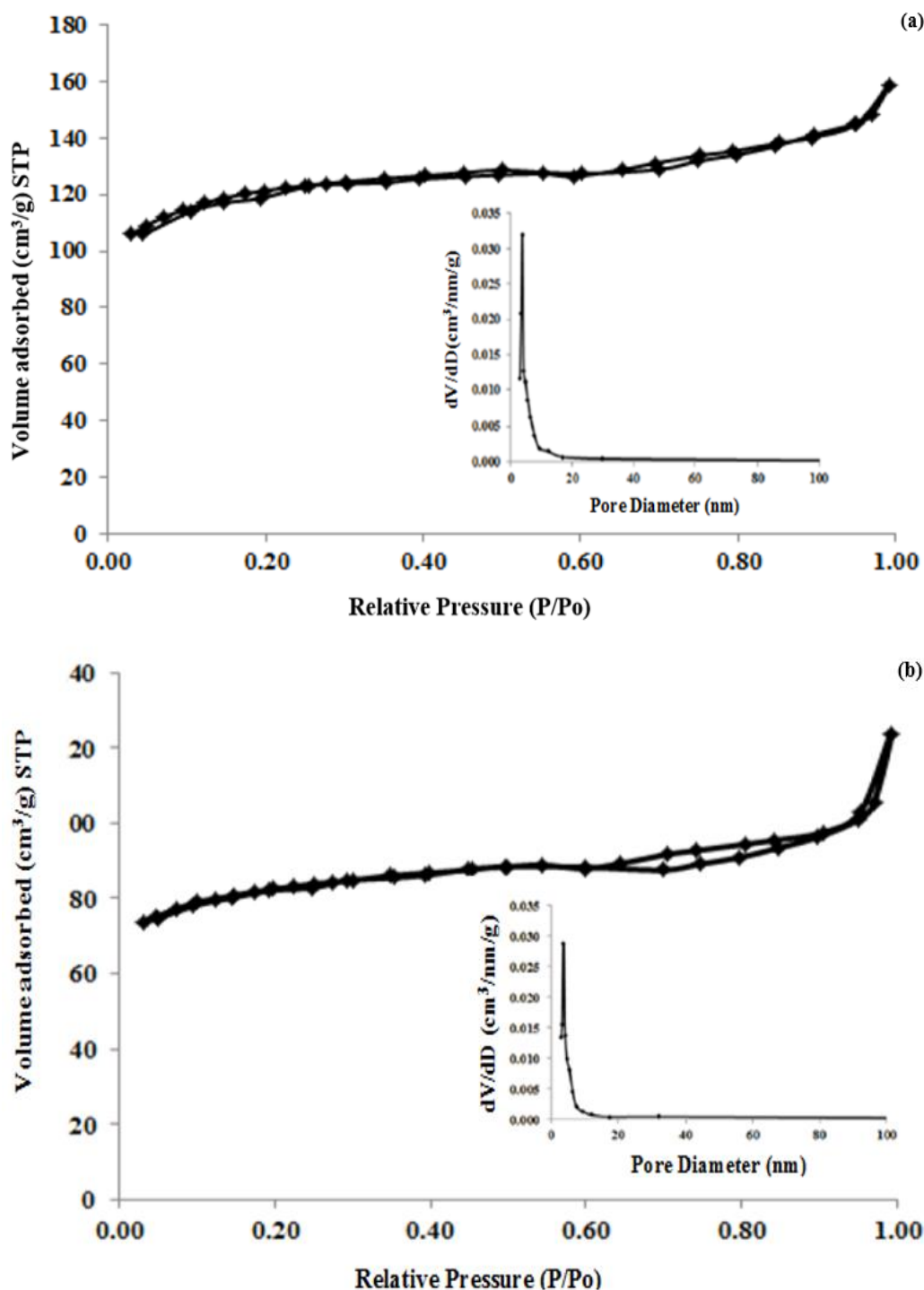


Figure 3. Nitrogen adsorption and desorption and BJH pore size distribution of catalyst. (a) HZSM-5; (b) Ni(5.42%)-Zn(1.11%)/HZSM-5 catalyst.

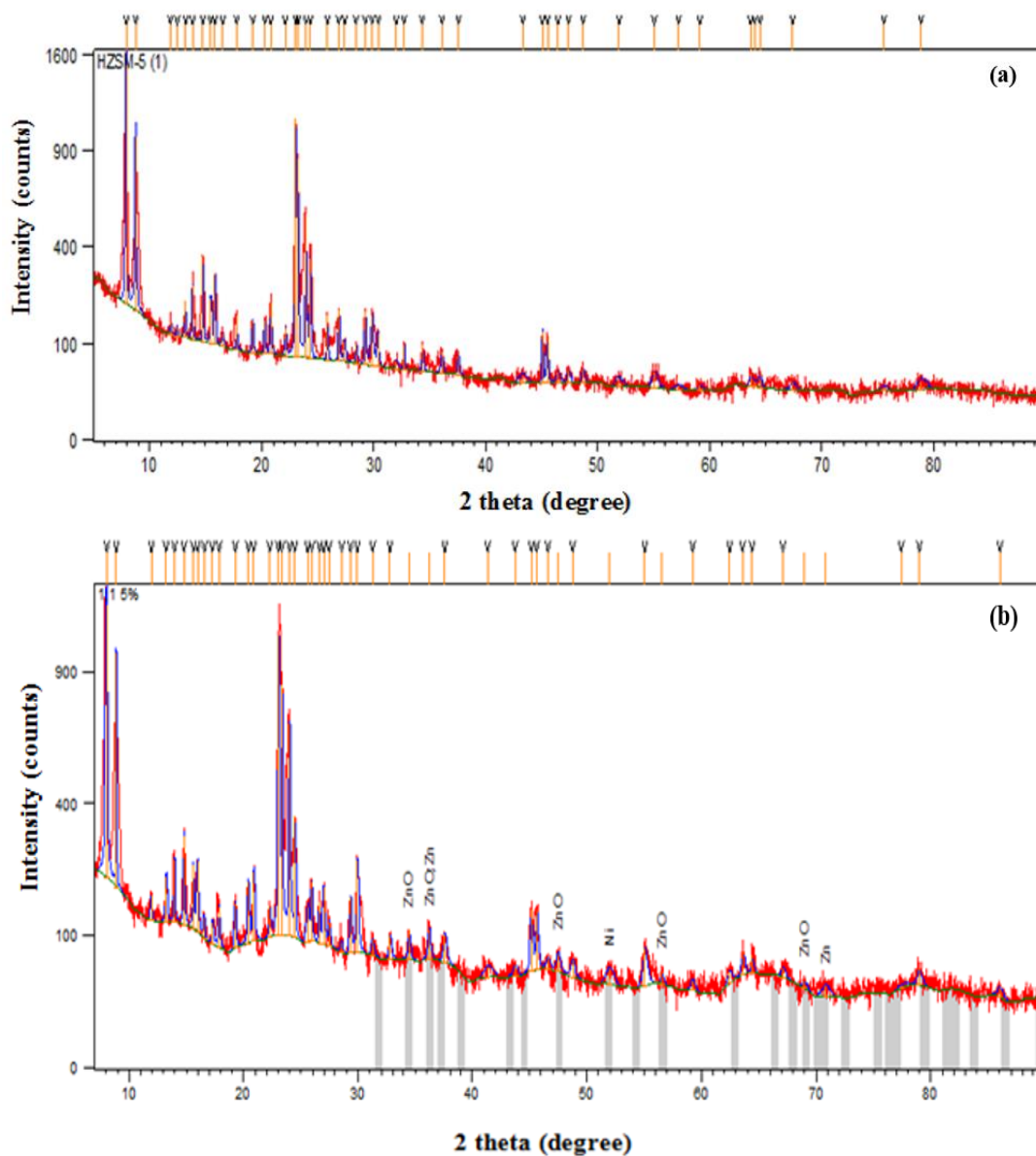
The pore size distributions of the two types of the catalyst were centered at 3.8 nm. However, the slightly narrower pore size distribution and lower peak height were seen on Ni-Zn impregnated on HZSM-5. Reduction of peak height on the catalyst showed that the presence of Ni and Zn had a considerable influence

on the pore structure of HZSM-5. Both of the catalysts have a mesoporous structure as the result of the interparticle voids. This pore structure will greatly affect the increase of reactivity of the catalysts, as reported by Wang *et al.* (2013).

Table 1 shows that micropores volume decreased from 0.156 to 0.101 cm³ g⁻¹, while pore diameter increased from 2.709 to 3.109 nm after Ni–Zn metals were impregnated on HZSM-5. Nevertheless, Chen *et al.* (2016) stated that the internal nickel particles can inhibit the nitrogen molecules into the pore by blocking the micropores of HZSM-5. However, the increase of pore diameter and the presence of mesopores size distribution indicated that fatty acids had a significant probability to diffuse into the pores successfully and react on the active sites. According to Bockisch (1998), assuming a typical triglyceride molecule to have a spherical form, its diameter would be 1.5 nm. Therefore, if the fatty acids cannot diffuse and react with the active sites located in micropores channel, then these fatty acids will diffuse and react with the active

sites located in mesopores channel. While the actual metals content obtained were shown in Table 1.

X-ray diffraction data of catalyst system shows that the full diffractograms were recorded in the range 2θ° of 5–90 to see the diffraction peak of NiO, ZnO, Ni and Zn in the catalyst samples. The characteristic of diffraction peaks of commercial HZSM-5, as shown in Fig. 4a, located at 2θ of 7.9, 8.8, 23.09, 23.31, 23.69, 23.9 and 24.4°, which indicated a structure type mordenite framework inverted (MFI), as reported by a previous study (Marlinda *et al.*, 2016). As shown in Fig. 4b and c, diffractograms of catalyst used for the hydrocracking on *Cerbera manghas* oil were almost similar to those of commercial HZSM-5.



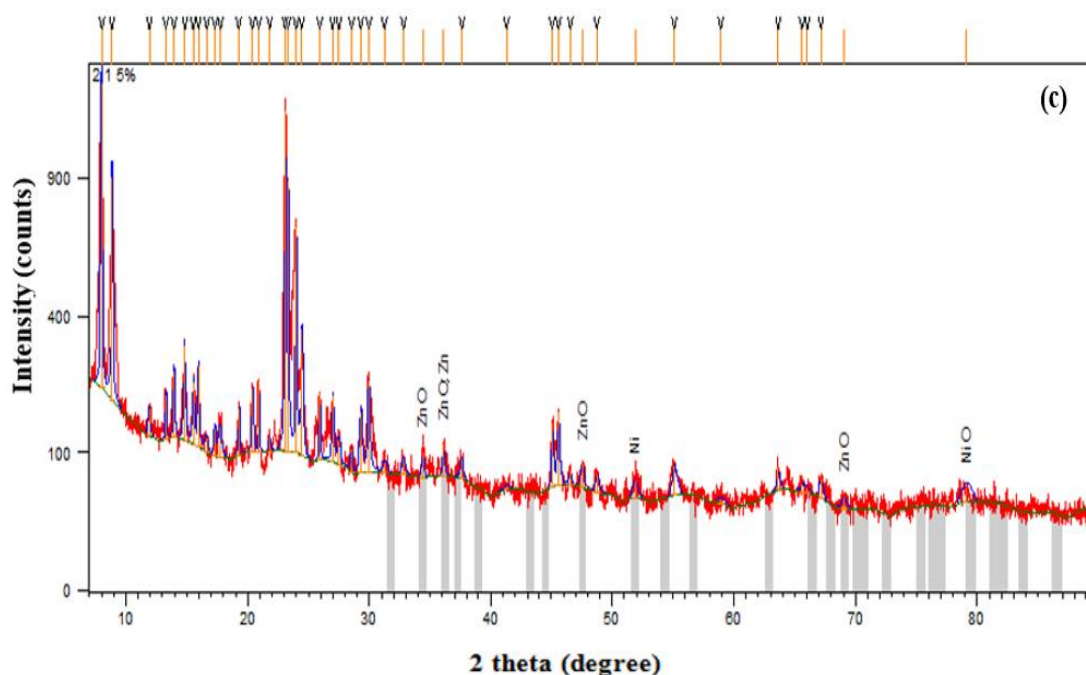


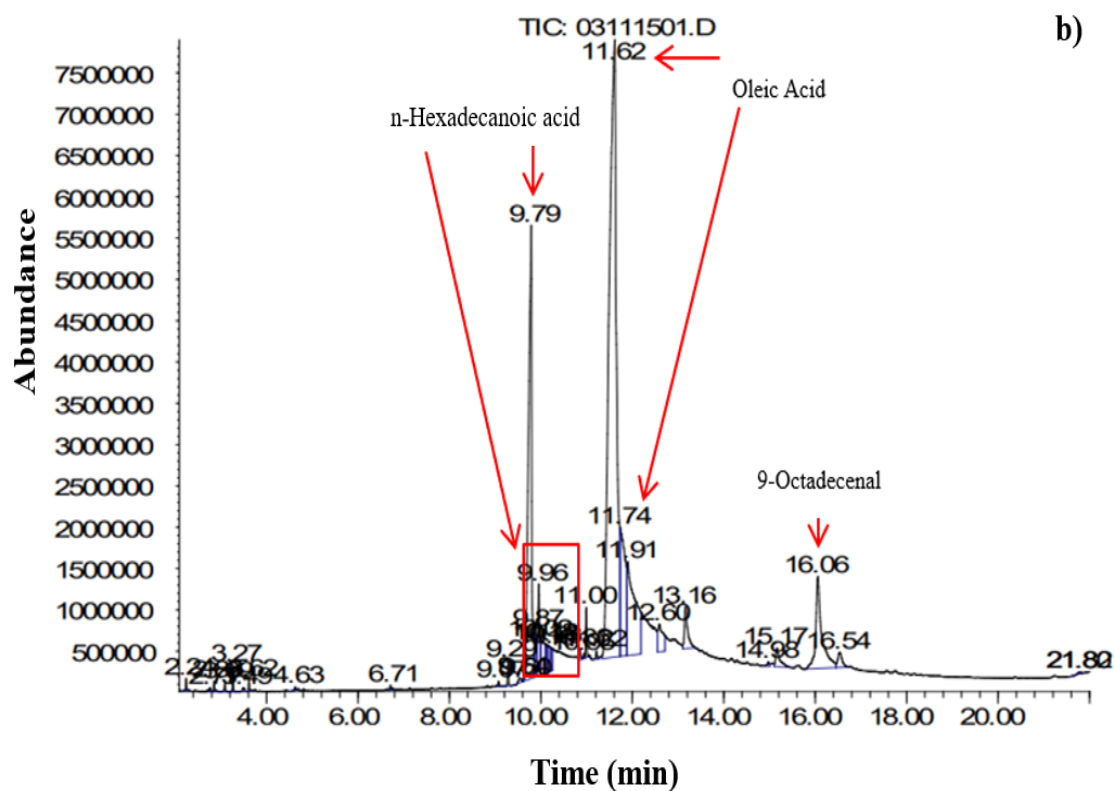
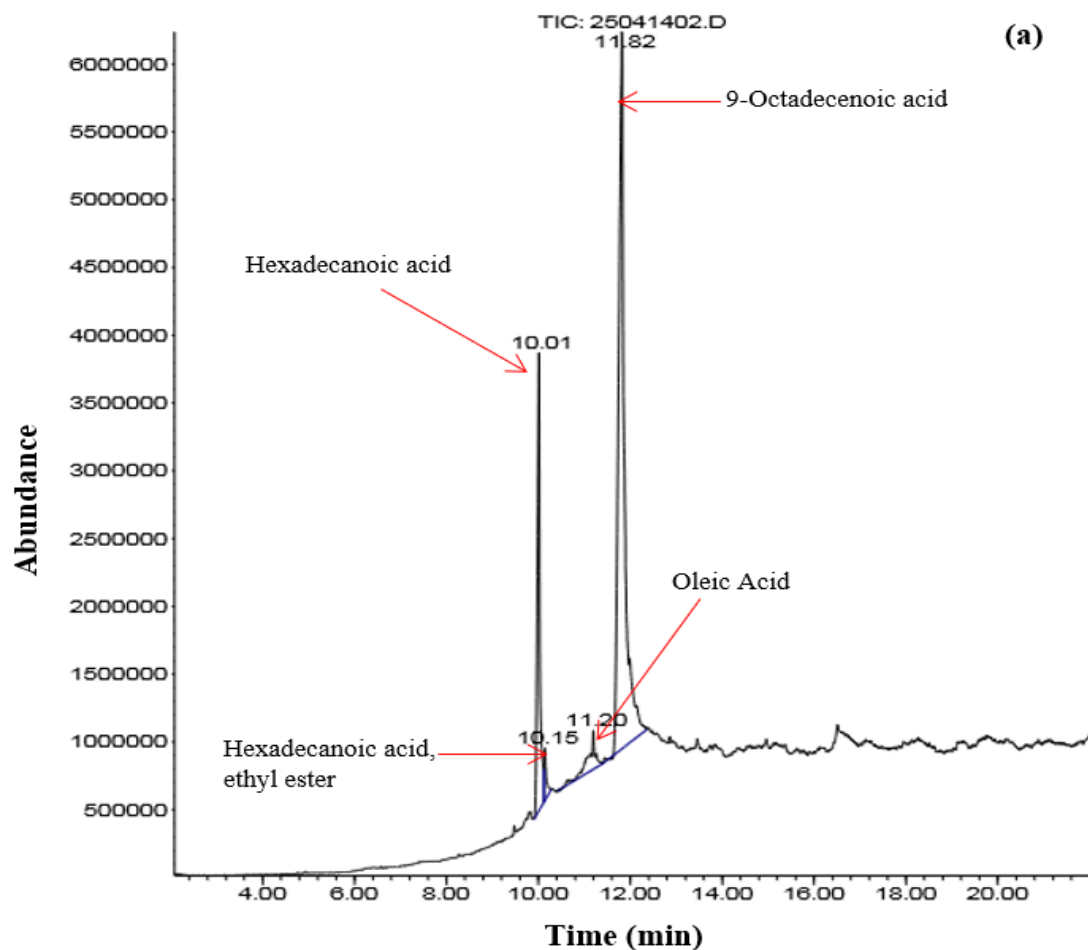
Figure 4. X-ray diffraction pattern of catalysts. (a) Commercial HZSM-5 after calcined (Marlinda *et al.*, 2016), (b) Ni(5.43%)-Zn(1.23%)/HZSM-5 catalyst, (c) Ni(5.42%)-Zn(1.11%)/HZSM-5 catalyst.

After impregnation with Ni–Zn, the HZSM-5 framework structure was almost unchanged, but only the intensity of each diffraction peak decreased (Chen *et al.*, 2016; Niu *et al.*, 2014; Wang *et al.*, 2013). Figure 4b shows that a small intensity diffraction peak of ZnO crystallites was observed at 2θ of 34.55, 36.32, 47.56, 56.66 and 69.08°. The Zn and Ni particles were also observed at 2θ of 70.94 and 52.06° with low intensity, respectively. While the presence of NiO crystallite was not found. Figure 4c shows that a small peak diffraction intensity of ZnO crystallites were observed at 2θ of 34.53, 36.19, 47.58 and 69.10°. NiO crystallite and Ni particle were observed at 2θ of 79.23 and 51.96° with low intensity, respectively. While the presence of Zn metal was not detected. When incipient wetness impregnation method was applied by means of physical mixing, diffraction peak for ZnO was obtained at 2θ of 36.21°, as observed by Niu *et al.* (2014). In principle, the reduction of ZnO and NiO crystallites with hydrogen will lead to the formation of proton ions (H^+), as the Bronsted acid. As reported by Chen *et al.* (2016), after reduction of NiO with hydrogen, proton ion (H^+)

was formed ($Ni^{2+} + H_2 \rightarrow Ni + 2H^+$) so that the catalysts which contained Bronsted acid sites (weak strength sites) have contributed to direct isomerization reaction. While Lewis acid sites (strong acid sites) may direct the ability of cracking.

3.3 Biofuel analysis

Biofuel produced from hydrocracking of *Cerbera manghas* oil at a temperature of 400 °C with a Ni-Zn(2%)/HZSM-5 catalyst and Ni-Zn(4%)/HZSM-5 (Prajitno *et al.*, 2015) still contained many carboxylic acids and compounds containing more oxygen, i.e., 9-octadecenal in the range of 5.35–6.11% and ethenone in the range of 0.20–0.37%. Table 3 shows that olefins are found in very small quantities while the n-paraffins and cycloparaffins can only be obtained from catalyst with metal loading of 4%. It indicated that the metals impregnated on HZSM-5 have not been able to hydrogenate fatty acid. The GC-MS spectra of biofuel is shown in Fig. 5.



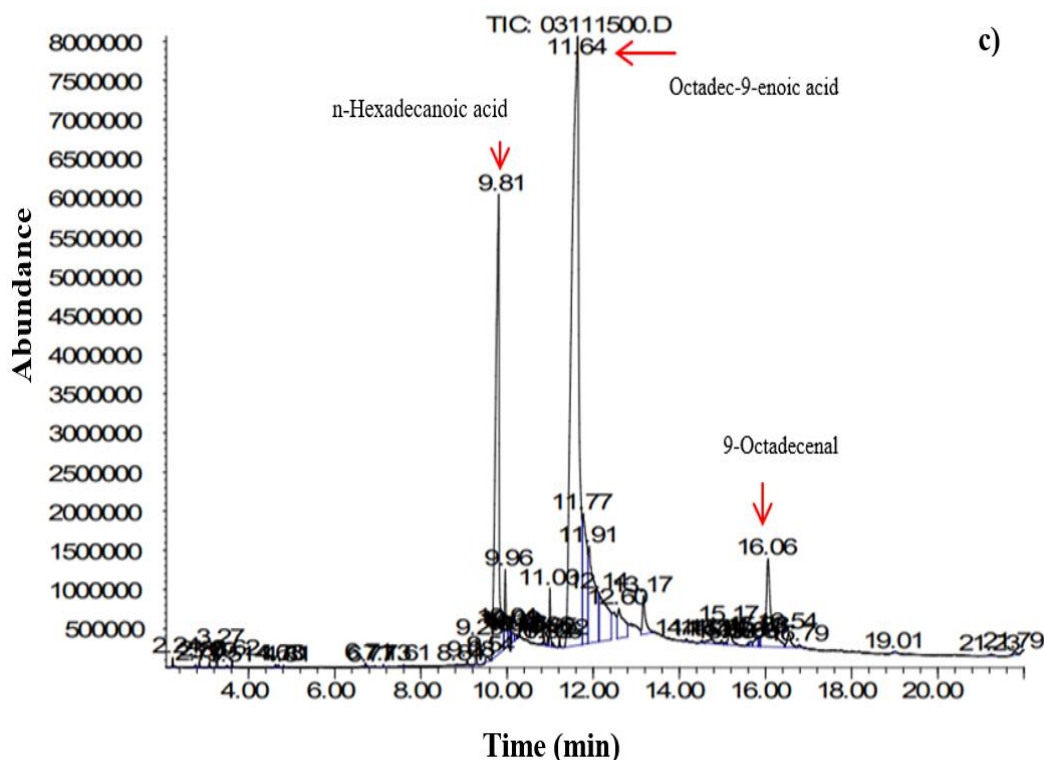


Figure 5. Gas chromatography-mass spectrometry spectra of (a) *Cerbera manghas* oil (Prajitno *et al.*, 2015), and liquid products produced at 400 °C with (b) Ni-Zn(2%)/HZSM-5 catalyst, (c) Ni-Zn(4%)/HZSM-5 catalyst, under pressure 20 ± 5 bar in the batch reactor.

Table 3. Hydrocarbon composition of biofuel produced by hydrocracking at temperature of 400 °C under pressure 20 bar in batch reactor, tested GC-MS.

| Catalyst | Hydrocarbon composition of biofuel (area%) | | | | | |
|------------------|--|---------------|----------|--------|-----------------|----------------------------|
| | n-paraffin | cycloparaffin | aromatic | olefin | carboxylic acid | Compound containing oxygen |
| Ni-Zn(2%)/HZSM-5 | 0 | 0 | 0 | 0.05 | 93.09 | 6.74 |
| Ni-Zn(4%)/HZSM-5 | 0.02 | 0.06 | 0 | 0.07 | 92.99 | 6.67 |

Gas chromatography-mass spectrometry spectra of *Cerbera manghas* oil and biofuel produced in the various reaction temperatures and metal loading of 5% are shown in Fig. 6 and 7, respectively. When Fig. 6 and 7 are compared, it can be seen that the compounds with retention time of 10–18 min in GC-MS spectra of *Cerbera manghas* oil disappear after reaction, as reported by a previous study (Marlinda *et al.*, 2016). It indicated that the triglycerides containing long chain

molecules were converted into short chain molecules by hydroprocessing (including cracking, deoxygenation, and isomerization reaction) with HZSM-5 catalyst, as reported by a previous study (Zheng *et al.*, 2015). Meanwhile, the number of different compounds with retention time of 0–9 min increased, as shown in Fig. 7. The presence of Ni and Zn metals have contributed to the hydrogenation process of unsaturated fatty acids into n-paraffins.

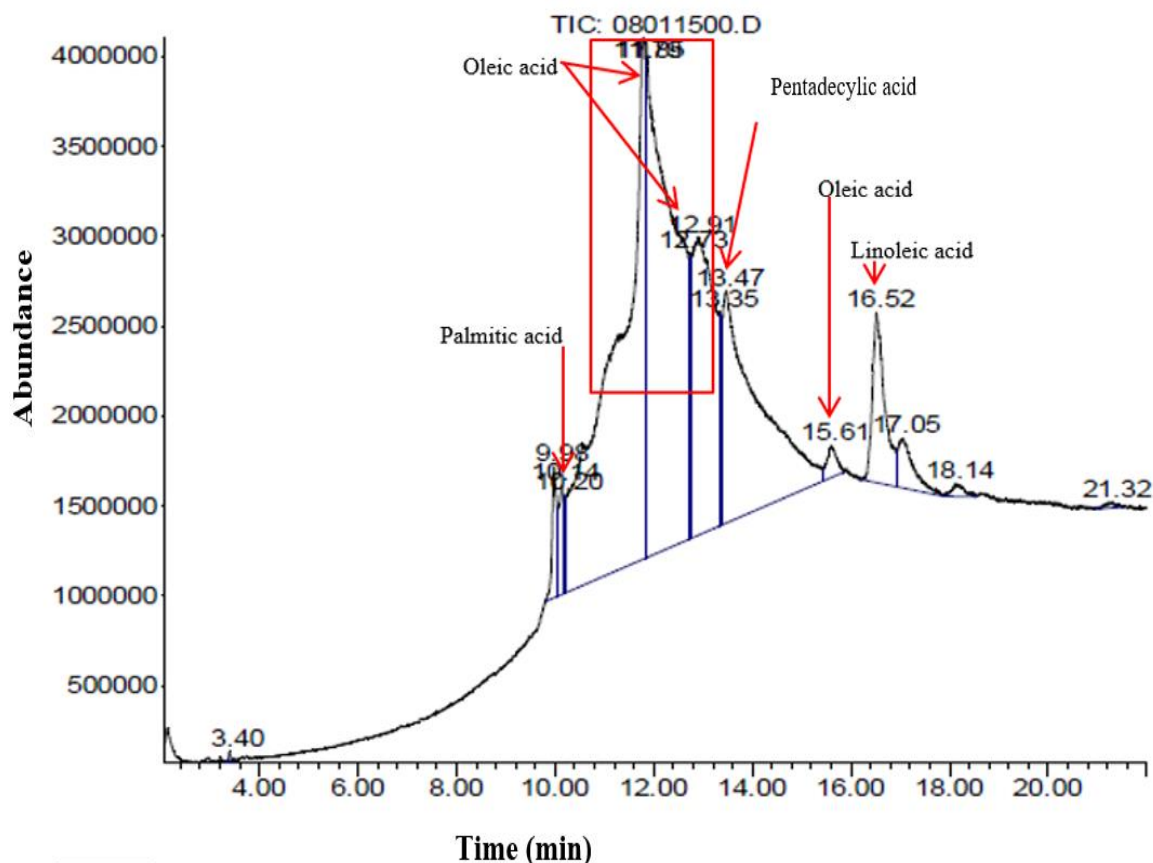
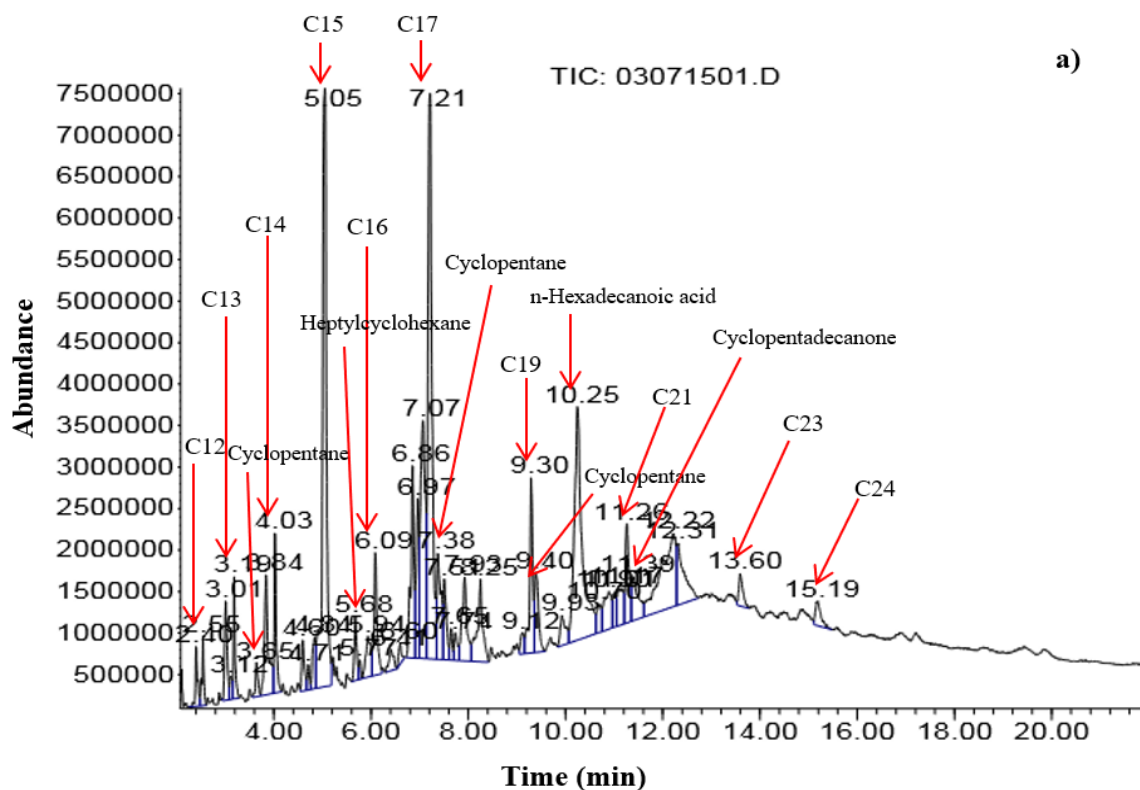
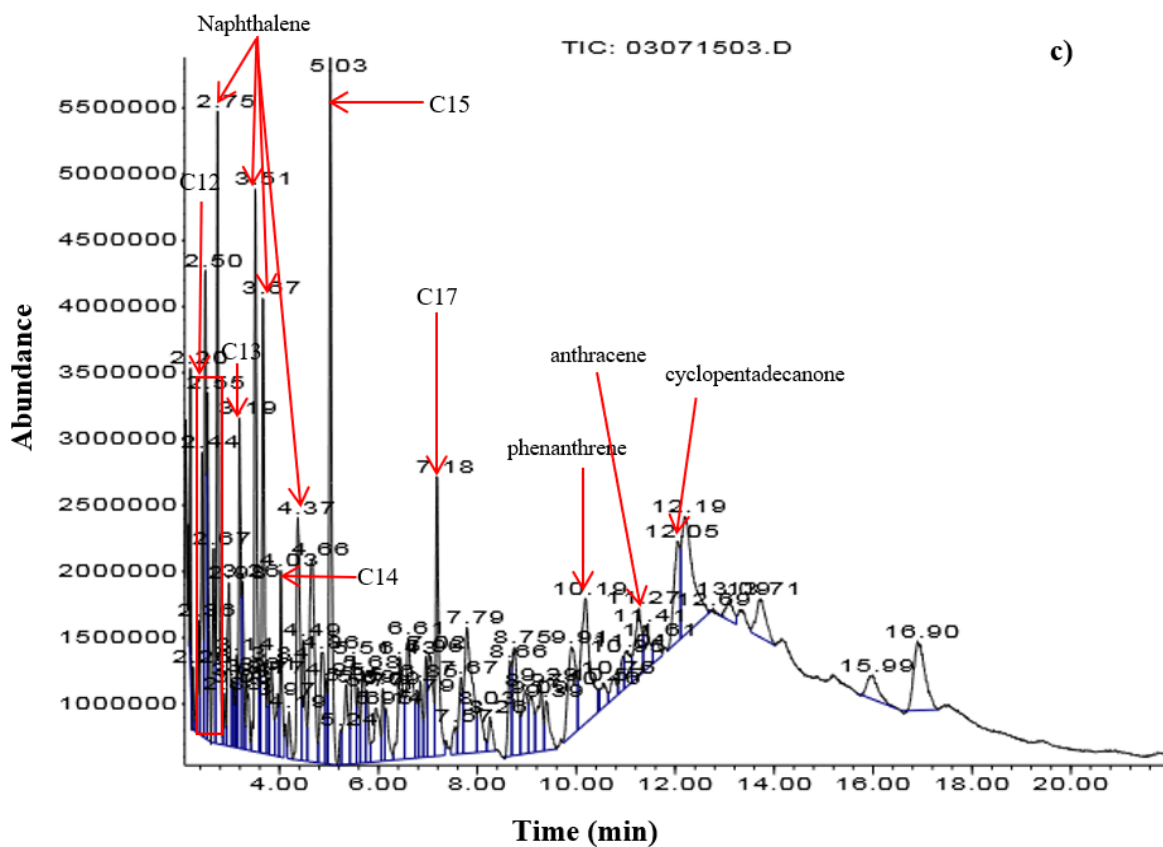
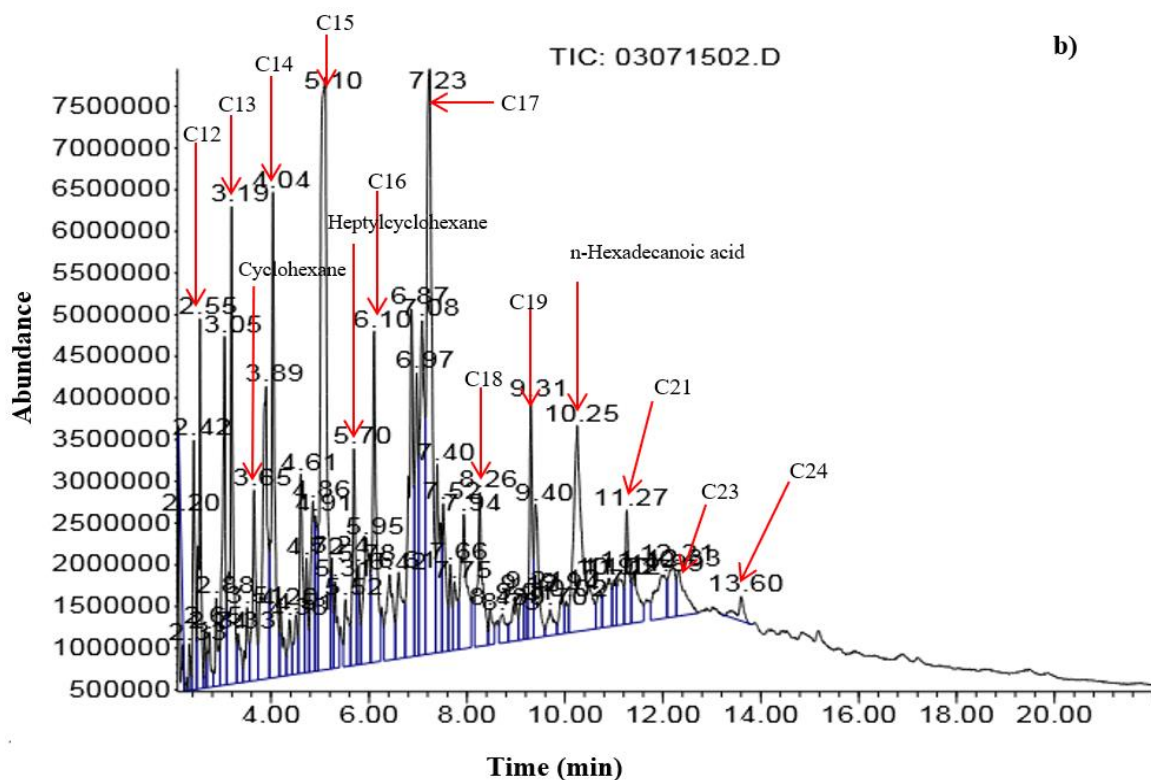
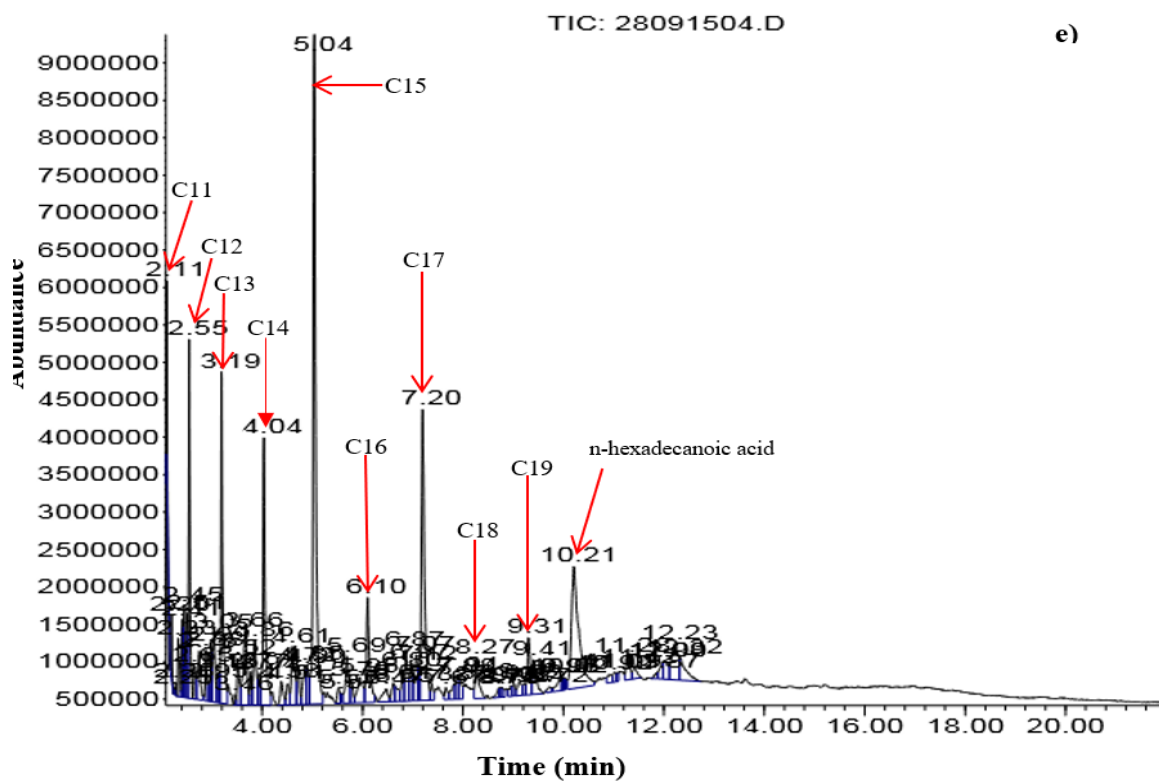
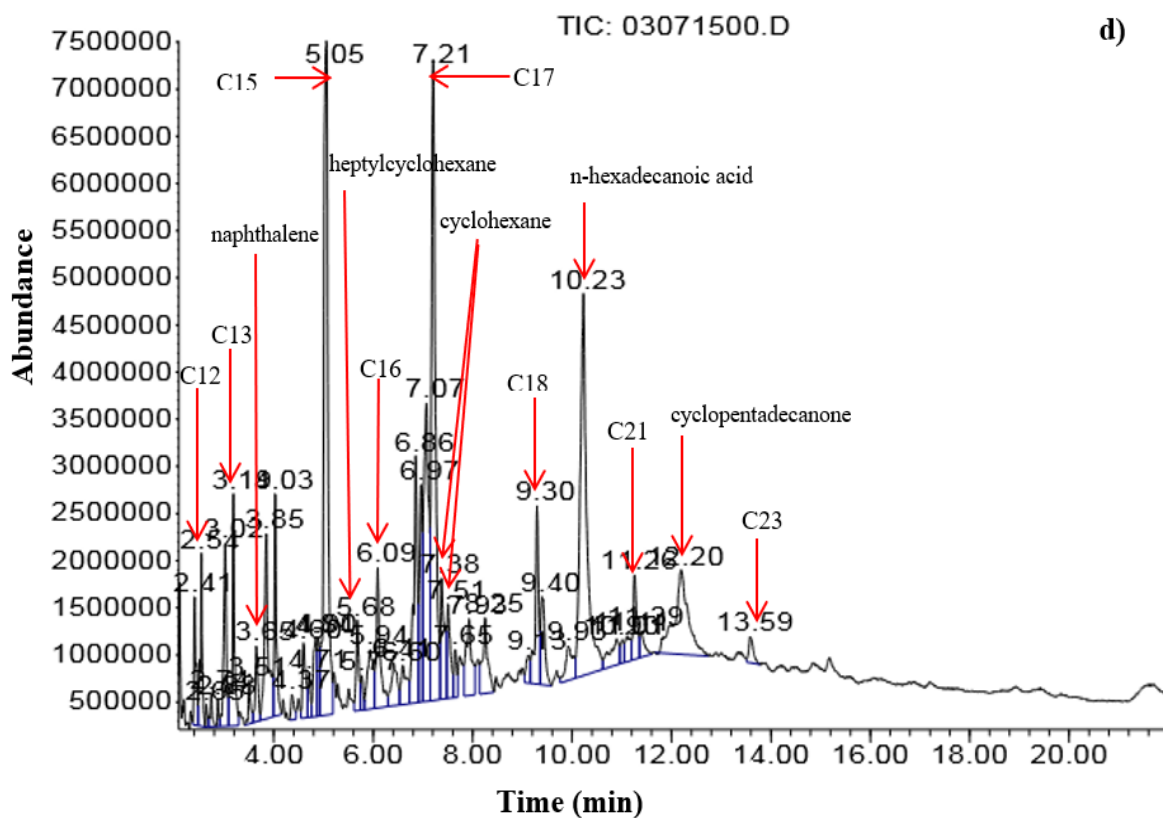


Figure 6. Gas chromatography-mass spectrometry spectra of *Cerbera manghas* oil.
 Source: Adapted from [Marlinda et al. \(2016\)](#).







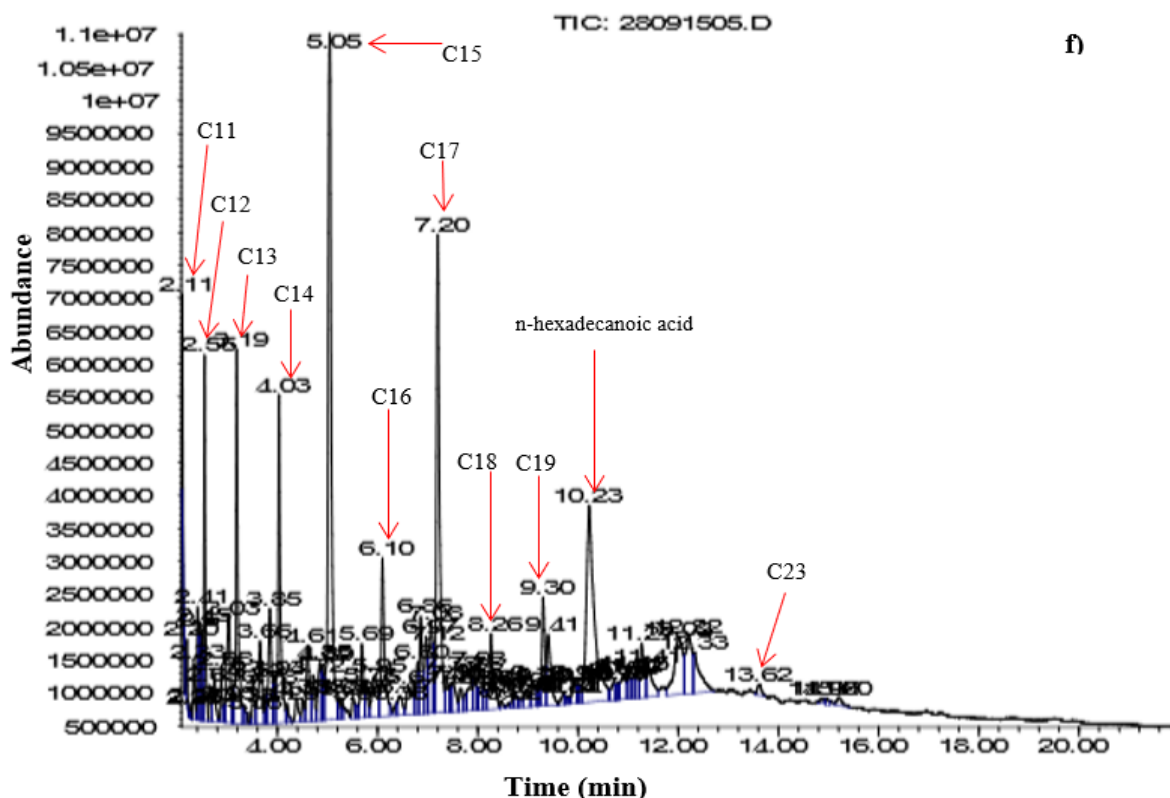


Figure 7. Gas chromatography-mass spectrometry spectra of biofuel produced at (a) 350 °C, (b) 375 °C, (c) 400 °C with Ni(5.43%)-Zn(1.23%)/HZSM-5 catalyst, and GC-MS spectra of biofuel produced at (d) 350 °C, (e) 375 °C, (f) 400 °C using Ni(5.42%)-Zn(1.11%)/HZSM-5 catalyst, under pressure 20 ± 5 bar in the batch reactor. Saturated chain hydrocarbons (n-paraffins) have the number of carbon atom from C12 to C24.

3.3.1 Effect of temperature on hydrocarbon composition

Figure 8a shows that biofuel contains a different hydrocarbon composition for each temperature of hydrocracking reactions with Ni(5.43%)-Zn(1.23%)/HZSM-5 catalyst. It can be seen that, at temperature of 350 °C, biofuel contained n-paraffins of 42.03 area%, but carboxylic acids of merely 15.48 area%, and compounds containing oxygen of 8.69 area%, i.e., octacosanol, were still found. Meanwhile, biofuel containing olefins of 20.31 area% and cycloparaffins of 12.48 area% was produced more at temperature of 375 °C. On the other hand, polycyclic aromatic hydrocarbons (PAHs) and aromatic are obtained at temperature of 400 °C, i.e., 21.32 and 35.47 area%, respectively. The existence of PAHs compounds

(including 1-methyl fluorene, phenanthrene, and anthracene) showed that the heating of vegetable oil was not complete. These compounds were not expected to present in biofuel. As reported by Vichaphund *et al.* (2015), deactivation occurred on HZSM-5 surface because of coke derived from PAHs compounds. Coke on the catalyst surface can be inhibited in the presence of hydrogen during hydrocracking reaction. However, overall, the compounds containing oxygen were still found in biofuel produced at all temperature variables. In principle, this compound should no longer exist in biofuel because the presence of oxygen atoms affects the viscosity and heating value, as reported by a previous study (Zheng *et al.*, 2015). Furthermore, isoparaffins were not found in biofuel for each reaction temperatures.

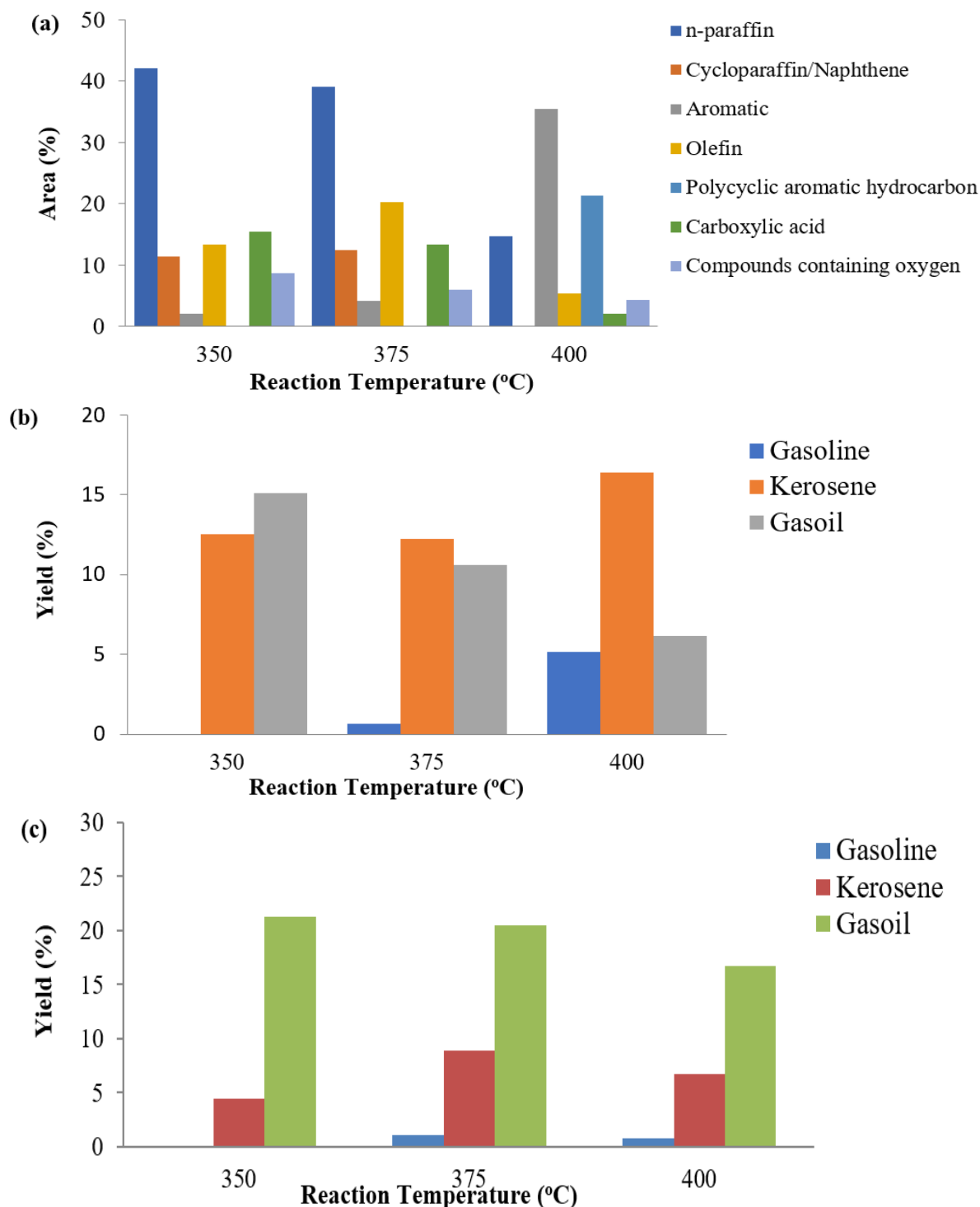


Figure 8. Effect of reaction temperature on (a) the hydrocarbon composition, (b) gasoline/kerosene/gasoil yields of liquid hydrocarbon fuel produced using Ni(5.43%)-Zn(1.23%)/HZSM-5 catalyst; (c) gasoline/kerosene/gasoil yields of liquid hydrocarbon fuel produced using Ni(5.42%)-Zn(1.11%)/HZSM-5 catalyst, under 20 bar in the batch reactor (“c” is elaborated by a previous study (Roesyadi *et al.*, 2016)).

The cracking of olefins into lighter hydrocarbon compounds was shown by the decrease of olefin at temperatures from 350 to 400 °C, as reported by Kim *et al.* (2013). On the other hand, aromatic hydrocarbon

compounds, i.e., 1-methyl-2-(2-propenyl) benzene of 4.5 area%, 1-Methylnaphthalene of 4.79 area%, 1,6-dimethylnaphthalene of 3.39 area%, 1-ethylnaphthalene of 2.64 area% were found at a temperature

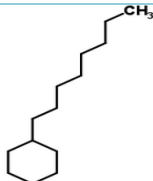
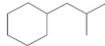
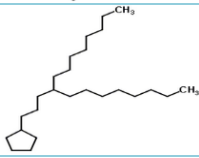
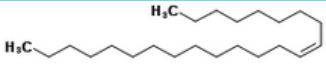
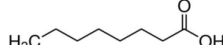
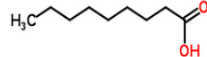
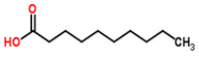
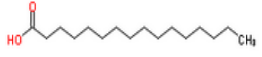
of 400 °C. In fact, aromatics increased with the increasing reaction temperature. This suggests that aromatization reaction on olefin occurred with the presence of HZSM-5 zeolite, as reported by Pinto *et al.* (2014). The cycloparaffins also indicated the functionality of acidic site on HZSM-5. As stated by a previous study (Chen *et al.*, 2016), the acidity of HZSM-5 zeolite decreased with the increase of active metal loading and Si/Al ratio. In addition, the H₂ to oil ratio would help the process of hydrogenation on olefins to n-paraffins. The determination of hydrocarbon composition and the degree of isomerization is useful to provide information to evaluate the properties of biofuel, such as cetane number (Kim *et al.*, 2013), freezing point, flash point and viscosity (Liu *et al.*, 2015).

Table 4 shows the components containing abundant compounds in biofuel based on group of hydrocarbons at a temperature of 350 °C. The main compound of cycloparaffin was cyclohexane with branched chain resulting in hydrogenation reaction of unsaturated hydrocarbon compounds, as found by Zheng *et al.* (2015). The n-hexadecanoic acid was formed greatly. It was indicated that the saturation of the double bond occurred quite well. The presence of oxygen-containing compounds showed that it would be better for hydrodeoxygenation reaction to occur at temperatures above 350 °C. Oxygen-containing compounds decreased from 8.69 to 4.33% at 350 and 400 °C, respectively. The increase of temperature led to the increasing cracking activity.

Table 4. Several abundant compounds in each group for biofuel produced at 350 °C, under 20 bar in the batch reactor* with Ni(5.43%)-Zn(1.23%)/HZSM-5 catalyst.

| Compounds | Area% | Structure |
|---|-------|-----------|
| Saturated chain hydrocarbon/n-paraffin | | |
| Dodecane/C ₁₂ H ₂₆ | 0.72 | |
| Tridecane/C ₁₃ H ₂₈ | 1.09 | |
| Tetradecane/C ₁₄ H ₃₀ | 1.78 | |
| Pentadecane/C ₁₅ H ₃₂ | 14.14 | |
| Hexadecane/C ₁₆ H ₃₄ | 2.06 | |
| Heptadecane/C ₁₇ H ₃₄ | 13.06 | |
| Octadecane/C ₁₈ H ₃₈ | 2.47 | |
| Nonadecane/C ₁₉ H ₄₀ | 3.05 | |
| Heneicosane/C ₂₁ H ₄₄ | 2.13 | |
| Tricosane | 0.76 | |
| Tetracosane | 0.77 | |
| Aromatic hydrocarbon | | |
| n-octylbenzene | 0.89 | |
| (5-Methyloctyl) benzene | 1.13 | |
| Cycloparaffin/Saturated naphthene | | |
| 1,1,3-trimethylcyclohexane | 2.36 | |
| Heptylcyclohexane | 3.18 | |
| 1-(cyclohexylmethyl)-2-methylcyclohexane | 0,5 | |
| Cyclohexane, 1-(1,5-dimethylhex. | 0.54 | |

Continue...

| | | |
|---|-------|---|
| n-octylcyclohexane | 0.76 |  |
| (2-methylpropyl) cyclohexane | 0.48 |  |
| (4-octyldodecyl) cyclopentane | 1.81 |  |
| Cyclotetradecane | 0.22 | |
| 1,7,11-trimethylcyclotetradecane | 1.27 | |
| Cyclopentadecane | 0.3 | |
| Olefin | | |
| 8-Heptadecene | 9.78 |  |
| 1-Heptadecene | 2.44 | |
| 9-Tricosene | 0.42 |  |
| 1-Hexacosene | 0.64 | |
| Carboxylic acid | | |
| Octanoic Acid | 0.72 |  |
| Nonanoic acid | 1.44 |  |
| 9-Octadecenoic acid | 0.34 |  |
| n-Decanoic Acid/ C ₁₀ H ₂₀ O ₂ | 2.7 |  |
| n-Hexadecanoic acid | 10.28 |  |
| Compounds containing oxygen | | |
| 3-methyl-2,6-dioxo-4-hexenoic acid | 0.9 | |
| Cyclopentadecanone | 1.59 |  |
| Octacosanol | 6.2 |  |

*Adopted from table format in literature [Zheng *et al.* \(2015\)](#).

As shown in [Tab. 4](#), the presence of pentadecane (C₁₅) and heptadecane (C₁₇) indicated that HDC was the more dominant reaction pathway than HDO. Although two of these reactions allowed the formation of n-paraffin, but the H₂ supplied for both reaction routes was different so that n-paraffin produced was different based on the number of carbons ([Pinto *et al.*, 2014](#); [Sotelo-Boyás *et al.*, 2012](#); [Zheng *et al.*, 2015](#)). Hydrogenation process on *Cerbera manghas* oil containing tripalmitin proceeded to obtain three palmitic acids and propane. By following the route of decarboxylation and/or decarbonylation without going through the saturation of the first double bond by hydrogenation reaction, pentadecane (C₁₅H₃₂) was

immediately produced. In fact, the highest triglycerides in *Cerbera manghas* oil were triolein. Triolein was hydrogenated to obtain three oleic acids and propane. It still contained a double bond, so the hydrogenation process on oleic acid into stearic acid occurred. By following the route of decarboxylation and/or decarbonylation, stearic acid was converted into heptadecane (C₁₇H₃₆). Furthermore, the aromatic compounds were produced through dehydrogenation process on olefin, i.e., the cracking and aromatization reactions as reported by [Zheng *et al.* \(2015\)](#).

With Ni(5.42%)-Zn(1.11%)/HZSM-5 catalyst, the highest yield for n-paraffin was found at a temperature of 375 °C. On the other hand, isoparaffin reaches the

highest value of 4.58 area% at 400 °C (Roesyadi *et al.*, 2016). A single type of methyl isomer was obtained as isomerization product at 400 °C, as shown in Tab. 5. This is similar to the result obtained by Chen *et al.* (2016), who reported that the short-branched isoparaffins were formed because methyl alkanes can pass easily through the HZSM-5 pore. Ethyl isomers

cannot be found because the molecular size of ethyl alkanes is larger than that of methyl alkanes. Isoparaffin increased significantly with the increasing reaction temperature because the literature (Chen *et al.*, 2016) stated that isomerization reaction proceeded in endothermic condition.

Table 5. Several abundant compounds in each group for biofuel produced at 400 °C, under 20 bar in the batch reactor*, using Ni(5.42%)-Zn(1.11%)/HZSM-5 catalyst.

| Compounds | Area% | Structure |
|---|-------|-----------|
| Saturated chain hydrocarbon/n-paraffin | | |
| Undecane/C ₁₁ H ₂₄ | 0.48 | |
| Dodecane/C ₁₂ H ₂₆ | 2.84 | |
| Tridecane/C ₁₃ H ₂₈ | 4.2 | |
| Tetradecane/C ₁₄ H ₃₀ | 4.45 | |
| Pentadecane/C ₁₅ H ₃₂ | 13.17 | |
| Hexadecane/C ₁₆ H ₃₄ | 2.91 | |
| Heptadecane/C ₁₇ H ₃₄ | 8.85 | |
| Octadecane/C ₁₈ H ₃₈ | 1.7 | |
| Nonadecane/C ₁₉ H ₄₀ | 1.42 | |
| Tricosane | 0.27 | |
| Isoparaffin | | |
| 3-Methylheptadecane | 1.72 | |
| 6,9-Dimethyltetradecane | 0.9 | |
| 2,6,10,14-Tetramethyloctadecane | 1.58 | |
| 3,8-Dimethyldecane | 0.38 | |
| Aromatic hydrocarbon | | |
| Phenyloctane /N-Octylbenzene | 1.03 | |
| Nonylbenzene | 1.31 | |
| Pentylbenzene | 0.78 | |
| (1,3-Dimethylbutyl) Benzene | 0.31 | |
| 1-Methyl-2-N-Hexylbenzene | 0.57 | |
| 1-Methylnaphthalene | 2.22 | |
| 2-Ethyl-naphthalene | 0.66 | |
| 1-Ethyl-2,3-dimethylbenzene/o-Xylene | 0.05 | |

Continue...

| | | |
|---|------|--|
| 2-methyl-1-propenylbenzene | 0.39 | |
| Cycloparaffin/Saturated naphthene | | |
| n-Nonylcyclohexane | 1.26 | |
| 1-(1,5-Dimethylhexyl)-4-(4-methyl pentyl) cyclohexane | 3.42 | |
| 1-Hexyl-3-methylcyclopentane | 0.54 | |
| (4-Methylpentyl) cyclohexane | 0.46 | |
| 1,2-Dicyclohexylethane | 1.35 | |
| 1,1,3-Trimethylcyclohexane | 0.62 | |
| 7-cyclohexyltridecane | 0.11 | |
| Dicyclohexylmethane | 0.68 | |
| 2,3-Dihydro-4-methyl-1H-indene | 0.7 | |
| Olefin | | |
| 8-Heptadecene | 4.66 | |
| 1-Heptadecene | 0.48 | |
| 1-Docosene | 0.13 | |
| Carboxylic acid | | |
| Octanoic Acid | 0.95 | |
| Nonanoic acid | 2.12 | |
| n-Decanoic Acid/ C ₁₀ H ₂₀ O ₂ | 2 | |
| n-Hexadecanoic acid/palmitat acid | 8.74 | |
| Tetradecanoic acid | 2.09 | |
| Compounds containing oxygen | | |
| 2-Nonadecanone | 1 | |
| 2-hydroxydodecanoic acid ethyl ester | 0.35 | |
| 2-Heptadecanone/Methyl pentadecyl ketone | 1.66 | |
| beta-octyl acrolein | 0.7 | |
| 1-Oxa-2-cyclohexadecanone | 0.37 | |

*Adopted from table format in literature Zheng *et al.* (2015).

With the increasing reaction temperature, aromatics increased significantly so that n-paraffin (including C15 and C17) and cycloparaffins also decreased for

Ni(5.43%)-Zn(1.23%)/HZSM-5 catalyst (Fig. 8a). It indicated that aromatization and cyclization reaction were favored at temperatures over 350 °C (Rocha Filho

et al., 1993). According to Šimáček *et al.* (2009; 2011), aromatics also increased because of the increasing cyclization reactions rate. Tamiyakul *et al.* (2016) also reported that the presence of Zn²⁺ and ZnO detected in HZSM-5 was responsible for n-paraffins dehydrogenation and oxygenates decarboxylation, respectively. As a result, more aromatic yield was produced.

3.3.2 Effect of temperature on gasoline/kerosene/gasoil yields

Gas chromatography-mass spectrometry spectra of biofuel produced was compared to the GC-MS spectra of petroleum fuel (Rasyid *et al.*, 2015). The liquid product was identified based on hydrocarbon compounds obtained from the GC-MS analysis. Then, the identified hydrocarbon was grouped as gasoline-like hydrocarbon (C5-C9), kerosene-like hydrocarbon (C10-C13), and gasoil-like hydrocarbon (C14-C22), as reported by Barrón *et al.* (2011). Figure 8b shows gasoline/kerosene/gasoil yields for biofuel produced over Ni(5.43%)-Zn(1.23%)/HZSM-5 catalyst, with reaction temperatures in the range of 350–400 °C.

As confirmed by Fig. 8b data, the various reaction temperatures will affect gasoil/kerosene yields. As a result, gasoil yield decreased, and kerosene yield increased with the increase of temperature. This suggests that the decline in the yield of gasoil due to hydrocracking of long chain hydrocarbons into shorter chain was random reaction mechanism, as reported in a previous study (Kim *et al.*, 2013). It is also presented in Fig. 8b that the highest gasoline and kerosene yields were obtained at 400 °C at 5.13 and 16.42%, respectively. Meanwhile, gasoil yield of 15.12% was obtained at 350 °C. Gasoil decreased with the increase of reaction temperature for two type catalyst, which can be seen in Fig. 8b and c.

If Fig. 8b and c are compared based on the yield of gasoil, the characteristic performance of the Ni(5.42%)-Zn(1.11%)/HZSM-5 catalyst is higher than that of the Ni(5.43%)-Zn(1.23%)/HZSM-5 catalyst. The Ni(5.43%)-Zn(1.23%)/HZSM-5 catalyst leads to the formation of gasoline and kerosene with increasing temperature. For the Ni(5.43%)-Zn(1.23%)/HZSM-5 catalyst, liquid hydrocarbon products in the kerosene range have been produced at 350 °C with several abundant compounds shown in Tab. 4. For Ni(5.42%)-Zn(1.11%)/HZSM-5, liquid hydrocarbon products in the kerosene/gasoline range were only produced at 400 °C with several abundant compounds, as shown in Tab. 5.

Differences in reaction temperature affect the constituent of hydrocarbons in biofuel produced. With Ni(5.43%)-Zn(1.23%)/HZSM-5 catalyst, at a temperature of 350 °C kerosene contained n-paraffin, i.e., dodecane, n-octylcyclohexane, n-octylbenzene, and pentadecane, while gasoil contained hydrocarbon compound, i.e., heptadecane, octadecane, nonadecane, heneicosane, (5-Methyloctyl) benzene, heptylcyclohexane, 1-(cyclohexylmethyl)-2-methylcyclohexane, and cyclopentadecane. Meanwhile, at reaction temperature of 400 °C, the higher gasoline yield was obtained with composition, i.e., 1,3-diethyl-5-methylbenzene, 1-methyl-2-(2-propenyl) benzene, 1,4-dimethyl-dihydro-azulene, and 1-methyl-3-(1-methylethyl) benzene. In principle, the presence of aromatics increases octane number in gasoline. Previously, the hydrocracking of *Calophyllum inophyllum* oil has been done to produce gasoline of 25.63%, kerosene of 17.31% and gasoil of 38.59% with CoMo(10%)/ γ -Al₂O₃ catalyst at 350 °C under pressure of 30 bar (Rasyid *et al.*, 2015).

4. Conclusions

The influence of the reaction temperature in hydrocracking on *Cerbera manghas* oil into biofuel with a catalyst Ni-Zn/HZSM-5 has been studied. The amount of n-paraffin decreased with the increasing temperature and followed by the increase of cycloparaffins and aromatics. This increasing reaction temperature led to an increase in the activity of cracking on a longer carbon chain molecule into a shorter carbon chain molecule. With Ni(5.43%)-Zn(1.23%)/HZSM-5 catalyst, highest kerosene was obtained at a temperature of 400 °C. At the same temperature, the higher isoparaffins contained the short-branched isoalkanes in gasoil were detected when the Ni(5.42%)-Zn(1.11%)/HZSM-5 catalyst was used. Therefore, reaction routes during hydrocracking are influenced by the reaction temperature and catalyst composition of Ni-Zn/HZSM-5, which provides acid function and metal function.

Authors' contribution

Conceptualization: Marlinda, L.; Danawati, H. P.

Data curation: Marlinda, L.

Formal Analysis: Marlinda, L.

Funding acquisition: Marlinda, L.; Danawati, H. P.

Investigation: Marlinda, L.; Danawati, H. P.; Roesyadi, A.; Gunardi, I.; Mirzayanti, Y. W.; Al Muttaqii, M.; Budianto, A.

Methodology: Marlinda, L.; Danawati, H. P.; Roesyadi, A.; Al Muttaqii, M.

Project administration: Marlinda, L.; Budianto, A.

Resources: Roesyadi, A.

Software: Not applicable

Supervision: Danawati, H. P.; Roesyadi, A.; Gunardi, I.

Validation: Danawati, H. P.; Roesyadi, A.; Gunardi, I.; Budianto, A.

Visualization: Marlinda, L.

Writing – original draft: Marlinda, L.

Writing – review & editing: Marlinda, L.; Al Muttaqii, M.; Mirzayanti, Y. W.

Data availability statement

All data sets were generated or analyzed in the current study.

Funding

DIPA-PNBP LPPM Faculty of Science and Technology, Lecturer Research Scheme, University of Jambi Fiscal Year 2019 Number: SP-DIPA-042.01.2.400950/2019 dated December 5 2018, according to the Research Contract Agreement Number: B/628/UN21.18/ PT.01.03/2019 Date 07 May 2019.

Acknowledgments

We thank to Chemical Reaction Engineering Laboratory, Department of Chemical Engineering, Sepuluh Nopember Institute of Technology for all the support, resources, and mentorship they provided. We are also sincerely grateful to Muhammad Iqbal, Victor Purnomo, and Ricco Aditya Setiyo Wicaksono (the research team member) for their contribution in this work. Finally, we would like to thank the University of Jambi, for funding this project.

References

Arun, N.; Sharma, R. V.; Dalai, A. K. Green diesel synthesis by hydrodeoxygenation of bio-based feedstocks: Strategies for catalyst design and development. *Renew. Sustain. Energy Rev.* **2015**, *48*, 240–255. <https://doi.org/10.1016/j.rser.2015.03.074>

Ayodele, O. B.; Farouk, H. U.; Mohammed, J.; Uemura, Y.; Daud W. M. A. W. Hydrodeoxygenation of oleic acid into n- and iso-paraffin biofuel using zeolite supported fluor-oxalate modified molybdenum catalyst: Kinetics study. *J. Taiwan*

Inst. Chem. Eng. **2015**, *50*, 142–152. <https://doi.org/10.1016/j.jtice.2014.12.014>

Barrón, C. A. E.; Melo-Banda, J. A.; Dominguez, J. M. E.; Hernández, M. E.; Silva, R. R.; Reyes, T. A. I.; Meraz, M. M. A. Catalytic hydrocracking of vegetable oil for agrofuels production using Ni–Mo, Ni–W, Pt and TFA catalysts supported on SBA-15. *Catal. Today* **2011**, *166* (1), 102–110. <https://doi.org/10.1016/j.cattod.2011.01.026>

Bezergianni, S.; Dimitriadis, A.; Meletidis, G. Effectiveness of CoMo and NiMo catalysts on co-hydroprocessing of heavy atmospheric gas oil–waste cooking oil mixtures. *Fuel* **2014**, *125*, 129–136. <https://doi.org/10.1016/j.fuel.2014.02.010>

Bockisch, M. *Fats and Oils Handbook*; AOCS Press, **1998**. <https://doi.org/10.1016/B978-0-9818936-0-0.50003-2>

Budianto, A.; Prajitno, D. H.; Budhikarjono, K. Biofuel production from candlenut oil using catalytic cracking process with Zn/HZSM-5 catalyst. *ARPN J. Eng. Appl. Sci.* **2014a**, *9* (11), 2121–2124.

Budianto, A.; Danawati H. P.; Roesyadi, A.; Budhikarjono, K. HZSM-5 catalyst for cracking palm oil to biodiesel: A Comparative study with and without Pt and Pd impregnation. *Scientific Study & Research: Chemistry & Chemical Engineering, Biotechnology, Food Industry* **2014b**, *15* (1): 81–90.

Carlier, J.; Guitton, J.; Bévalot, F.; Fanton, L.; Gaillard. Y. The principal toxic glycosidic steroids in *Cerbera manghas* L. seeds: Identification of cerberin, neriifolin, tanghinin and deacetyltanghinin by UHPLC–HRMS/MS, quantification by UHPLC–PDA-MS. *J. Chromatogr. B* **2014**, *962*, 1–8. <https://doi.org/10.1016/j.jchromb.2014.05.014>

Chen, X.; Dong, M.; Niu, X.; Wang, K.; Chen, G.; Fan, W.; Wang, J.; Qin, Z. Influence of Zn species in HZSM-5 on ethylene aromatization. *Chin. J. Catal.* **2015**, *36* (6), 880–888. [https://doi.org/10.1016/S1872-2067\(14\)60289-8](https://doi.org/10.1016/S1872-2067(14)60289-8)

Chen, L.; Li, H.; Fu, J.; Miao, C.; Lv, P.; Yuan, Z. Catalytic hydroprocessing of fatty acid methyl esters to renewable alkane fuels over Ni/HZSM-5 catalyst. *Catal. Today* **2016**, *259* (Part 2), 266–276. <https://doi.org/10.1016/j.cattod.2015.08.023>

Chuah, L. F.; Yusup, S.; Aziz, A. R. A.; Klemeš, J. J.; Bokhari, A.; Abdullah, M. Z. Influence of fatty acids content in non-edible oil for biodiesel properties. *Clean Techn. Environ. Policy* **2016**, *18*, 473–482. <https://doi.org/10.1007/s10098-015-1022-x>

Dwivedi, G.; Sharma, M. P. Application of Box-Behnken design in optimization of biodiesel yield from Pongamia oil and its stability analysis. *Fuel* **2015**, *145*, 256–262. <https://doi.org/10.1016/j.fuel.2012.03.019>

- Haber, J.; Block, J. H.; Delmon, B. Manual of methods and procedures for catalyst characterization. *Pure & Appl. Chem.* **1995**, *67* (Nos 8/9), 1257–1306. <https://doi.org/10.1351/pac199567081257>
- Hao, K.; Shen, B.; Wang, Y.; Ren, J. Influence of combined alkaline treatment and Fe–Ti-loading modification on ZSM-5 zeolite and its catalytic performance in light olefin production. *J. Ind. Eng. Chem.* **2012**, *18* (5), 1736–1740. <https://doi.org/10.1016/j.jiec.2012.03.019>
- Isahak, W. N. R. W.; Hisham, M. W. M.; Yarmo, M. A.; Hin, T.-y. Y. A review on bio-oil production from biomass by using pyrolysis method. *Renew. Sustain. Energy Rev.* **2012**, *16* (8), 5910–5923. <https://doi.org/10.1016/j.rser.2012.05.039>
- Ishihara, A.; Fukui, N.; Nasu, H.; Hashimoto, T. Hydrocracking of soybean oil using zeolite-alumina composite supported NiMo catalyst. *Fuel* **2014**, *134*, 611–617. <https://doi.org/10.1016/j.fuel.2014.06.004>
- Kim, S. K.; Brand, S.; Lee, H.-s.; Kim, Y.; Kim, J. Production of renewable diesel by hydrotreatment of soybean oil: Effect of reaction parameters. *Chem. Eng. J.* **2013**, *228*, 114–123. <https://doi.org/10.1016/j.cej.2013.04.095>
- Li, L.; Quan, K.; Xu, J.; Liu, F.; Liu, S.; Yu, S.; Xie, C.; Zhang, B.; Ge, X. Liquid hydrocarbon fuels from catalytic cracking of rubber seed oil using USY as catalyst. *Fuel* **2014**, *123*, 189–193. <https://doi.org/10.1016/j.fuel.2014.01.049>
- Liu, S.; Zhu, Q.; Guan, Q.; He, L.; Li, W. Bio-aviation fuel production from hydroprocessing castor oil promoted by the nickel-based bifunctional catalysts. *Bioresour. Technol.* **2015**, *183*, 93–100. <https://doi.org/10.1016/j.biortech.2015.02.056>
- Lu, Q.; Li, W.-Z.; Zhu, X.-F. Overview of fuel properties of biomass fast pyrolysis oils. *Energy Convers. Manag.* **2009**, *50* (5), 1376–1383. <https://doi.org/10.1016/j.enconman.2009.01.001>
- Marlinda, L.; Al-Muttaqii, M.; Roesyadi, A.; Prajitno, D. H. Production of biofuel by hydrocracking of *Cerbera manghas* oil using Co-Ni/HZSM-5 catalyst: Effect of reaction temperature. *J. Pure Appl. Chem. Res.* **2016**, *5* (3), 189–195. <https://doi.org/10.21776/ub.jpacr.2016.005.03.254>
- Niu, X.; Gao, J.; Miao, Q.; Dong, M.; Wang, G.; Fan, W.; Qin, Z.; Wang, J. Influence of preparation method on the performance of Zn-containing HZSM-5 catalysts in methanol-to-aromatics. *Microporous Mesoporous Mater.* **2014**, *197*, 252–261. <https://doi.org/10.1016/j.micromeso.2014.06.027>
- Pinto, F.; Martins, S.; Gonçalves, M.; Costa, P.; Gulyurtlu, I.; Alves, A.; Mendes, B. Hydrogenation of rapeseed oil for production of liquid bio-chemicals. *Appl. Energy* **2013**, *102*, 272–282. <https://doi.org/10.1016/j.apenergy.2012.04.008>
- Pinto, F.; Varela, F. T.; Gonçalves, M.; André Neto, R.; Costa, P.; Mendes, B. Production of bio-hydrocarbons by hydrotreating of pomace oil. *Fuel* **2014**, *116*, 84–93. <https://doi.org/10.1016/j.fuel.2013.07.116>
- Prajitno, D. H.; Roesyadi, A.; Budianto, A.; Iqbal, M.; Purnomo, V. Modification of Ni-Zn/HZSM-5 double promoted catalyst for biofuel production from *Cerbera manghas* oil. In Green Chemistry Section 1: Material Chemistry, *Proceedings of the 9th Joint Conference on Chemistry*, Semarang, Indonesia, November 12–13, 2014; Prajitno, D. H.; Roesyadi, A.; Budianto, A.; Iqbal, M.; Purnomo, V., Eds.; Diponegoro University: Semarang, **2015**; pp 25–28.
- Rasyid, R.; Prihartantyo, A.; Mahfud, M.; Roesyadi, A. Hydrocracking of *Calophyllum inophyllum* oil with non-sulfide CoMo catalysts. *Bull. Chem. React. Eng. Catal.* **2015**, *10* (1), 61–69. <https://doi.org/10.9767/bcrec.10.1.6597.61-69>
- Rocha Filho, G. N.; Brodzki, D.; Djéga-Mariadassou, G. Formation of alkanes alkylcycloalkanes and alkylbenzenes during the catalytic hydrocracking of vegetable oils. *Fuel* **1993**, *72* (4), 543–549. [https://doi.org/10.1016/0016-2361\(93\)90114-H](https://doi.org/10.1016/0016-2361(93)90114-H)
- Roesyadi, A.; Hariprajitno, D.; Nurjannah, N.; Savitri, S. D. HZSM-5 Catalyst for cracking palm oil to gasoline: A comparative study with and without impregnation. *Bull. Chem. React. Eng. Catal.* **2013**, *7* (3), 185–190. <https://doi.org/10.9767/bcrec.7.3.4045.185-190>
- Roesyadi, A. *Pembuatan Biofuel dari Minyak Nabati*; PT. Revka Petra Media, **2016**.
- Roesyadi, A.; Budianto, A.; Prajitno, D. H.; Gunardi, I.; Marlinda, L. Metode Pembuatan Katalis Ni-Zn/HZSM-5 untuk Produksi Biofuel dari Minyak Bintaro (*Cerbera manghas* Oil). ID, P00201607714, **2016**. <https://pdki-indonesia.dgip.go.id/detail/P00201607714?type=patent&keyword=bintaro> (accessed 2021-12-19).
- Romero, M. D.; Calles, J. A.; Rodríguez, A.; Cabanelas, J. C. The influence of calcination treatment over bifunctional Ni/HZSM-5 catalysts. *Ind. Eng. Chem. Res.* **1998**, *37* (10), 3846–3852. <https://doi.org/10.1021/ie980143i>
- Romero, M.; Pizzi, A.; Toscano, G.; Casazza, A. A.; Busca, G.; Bosio, B.; Arato, E. Preliminary experimental study on biofuel production by deoxygenation of *Jatropha* oil. *Fuel Process. Technol.* **2015**, *137*, 31–37. <https://doi.org/10.1016/j.fuproc.2015.04.002>

- Santillan-Jimenez E.; Crocker, M. Catalytic deoxygenation of fatty acids and their derivatives to hydrocarbon fuels via decarboxylation/decarbonylation. *J. Chem. Technol. Biotechnol.* **2012**, *87* (8), 1041–1050. <https://doi.org/10.1002/jctb.3775>
- Sartipi, S.; Parashar, K.; Valero-Romero, M. J.; Santos, V. P.; van der Linden, B.; Makkee, M.; Kapteijn, F.; Gascon, J. Hierarchical H-ZSM-5-supported cobalt for direct synthesis of gasoline-range hydrocarbon from syngas: Advantages, limitation, and mechanistic insight. *J. Catal.* **2013**, *305*, 179–190. <https://doi.org/10.1016/j.jcat.2013.05.012>
- Silva, V. T.; Sousa, L. A. Catalytic upgrading of fats and vegetable oils for the production of fuels. In *The role of catalysis for the sustainable production of bio-fuels and bio-chemicals*; Elsevier Science; **2013**, pp 67–92. <https://doi.org/10.1016/B978-0-444-56330-9.00003-6>
- Šimáček, P.; Kubička, D.; Šebor, G.; Pospíšil, M. Hydroprocessed rapeseed oil as a source of hydrocarbon-based biodiesel. *Fuel* **2009**, *88* (3), 456–460. <https://doi.org/10.1016/j.fuel.2008.10.022>
- Šimáček, P.; Kubička, D.; Kubičková, I.; Homola, F.; Pospíšil, M.; Chudoba, J. Premium quality renewable diesel fuel by hydroprocessing of sunflower oil. *Fuel* **2011**, *90*, 2473–2479. <https://doi.org/10.1016/j.fuel.2011.03.013>
- Sotelo-Boyás, R.; Trejo-Zárraga, F.; Hernández-Loyo, F. J. Hydroconversion of triglycerides into green liquid fuels. In *Hydrogenation*; IntechOpen, 2012; pp 187–216. <https://doi.org/10.5772/48710>
- Tamiyakul, S.; Anutamjarikun, S.; Jongpatiwut, S. The effect of Ga and Zn over HZSM-5 on the transformation of palm fatty acid distillate (PFAD) to aromatics. *Catal. Commun.* **2016**, *74*, 49–54. <https://doi.org/10.1016/j.catcom.2015.11.002>
- Vichaphund, S.; Aht-ong, D.; Sricharoenchaikul, V.; Atong, D. Production of aromatic compounds from catalytic fast pyrolysis of Jatropha residues using metal/HZSM-5 prepared by ion-exchange and impregnation methods. *Renew. Energy* **2015**, *79*, 28–37. <https://doi.org/10.1016/j.renene.2014.10.013>
- Vitale, G.; Molero, H.; Hernandez, E.; Aquino, S.; Birss, V.; Pereira-Almao, P. One-pot preparation and characterization of bifunctional Ni-containing ZSM-5 catalyst. *Appl. Catal. A: Gen.* **2013**, *452*, 75–87. <https://doi.org/10.1016/j.apcata.2012.11.026>
- Wang, S.; Yin, Q.; Guo, J.; Ru, B.; Zhu, L. Improved Fischer-Tropsch synthesis for gasoline over Ru, Ni promoted Co/HZSM-5 catalyst. *Fuel* **2013**, *108*, 597–603. <https://doi.org/10.1016/j.fuel.2013.02.021>
- Wang, C.; Liu, Q.; Song, J.; Li, W.; Li, P.; Xu, R.; Ma, H.; Tian, Z. High quality diesel-range alkanes production via a single-step hydrotreatment of vegetable oil over Ni/zeolite catalyst. *Catal. Today* **2014**, *234*, 153–160. <https://doi.org/10.1016/j.cattod.2014.02.011>
- Wu, L.; Guo, S.; Wang, C.; Yang Z. Production of alkanes (C₇–C₂₉) from different part of poplar tree via direct deoxy-liquefaction. *Bioresour. Technol.* **2009**, *100* (6), 2069–2076. <https://doi.org/10.1016/j.biortech.2008.10.024>
- Zhang, H.; Lin, H.; Zheng, Y. The role of cobalt and nickel in deoxygenation of vegetable oils. *Appl. Catal. B: Environ.* **2014**, *160–161*, 415–422. <https://doi.org/10.1016/j.apcatb.2014.05.043>
- Zheng, X.; Chang, J.; Fu, Y. One-pot catalytic hydrocracking of diesel distillate and residual oil fractions obtained from bio-oil to gasoline-range hydrocarbon fuel. *Fuel* **2015**, *157*, 107–114. <https://doi.org/10.1016/j.fuel.2015.05.002>